Electronic Supplementary Information

Well-defined multiblock poly(vinylidene difluoride) and block copolymers thereof: A missing piece of the architecture puzzle

Sanjib Banerjee,*,# Yogesh Patil, Olinda Gimello and Bruno Ameduri*

Ingénierie et Architectures Macromoléculaires, Institut Charles Gerhardt, UMR 5253 CNRS, UM, ENSCM, Place Eugène Bataillon, 34095 Montpellier Cedex 5, France

#Present address: Material Science and Technology Division, CSIR-National Institute for Interdisciplinary Science and Technology, Thiruvananthapuram 695019, Kerala, India

*Corresponding Authors: E-mail: bruno.ameduri@enscm.fr (B. Ameduri)

sanjibbanerjee@niist.res.in (S. Banerjee)

Contents:

1- Materials. All reagents were used as received unless stated otherwise. *tert*-Butyl-2-trifluoromethacrylate (MAF-TBE) was kindly offered by Tosoh F-Tech Company (Shunan, Japan). 1,1-Difluoroethylene (vinylidene fluoride, VDF) was kindly supplied by Arkema (Pierre Benite, France). Vinyl acetate (VAc, ≥99%, Aldrich) was stored under nitrogen and purged for 30 mins with nitrogen before use. 2-(Trifluoromethyl)oxirane (Apollo Scientific), carbon disulfide (Sigma-Aldrich), 2,2′-azobis (4-methoxy-2,4-dimethylvaleronitrile) (V-70, Wako), *tert*-amyl peroxy-2-ethylhexanoate (TAPE, 95%, AkzoNobel), and n-butylamine (n-$BuNH_2$, 99.5%, Aldrich) were used as received. Reagent Plus grade dimethyl carbonate (DMC, purity >99%), N,N-dimethylformamide (DMF, purity >99.8%), and laboratory reagent grade pentane (purity >95%) were purchased from Sigma-Aldrich and used as received. Deuterated acetone (acetone-d_6) and $CDCl_3$ used for NMR spectroscopy were purchased from Euroiso-top (Grenoble, France) (purity >99.8%).

2- Experimental Procedures.

2.1. Synthesis of cyclic xanthate (cy-XA). The cy-XA, 5-(trifluoromethyl)-1,3-oxathiolane-2-thione, TFOT, was synthesized by a previously reported procedure,[1] and characterized.

^{1}H NMR (400 MHz, $CDCl_3$, δ ppm, Fig. S1): 3.82 (AB system, $^2J_{HH}$ = 46 Hz, $^3J_{HH}$ = 7 Hz, 2H, –C<u>H</u>$_2$); 5.4 (X part of AB system, $^3J_{HF}$ = 7 Hz, $^3J_{HH}$ = 8 Hz, 1H, –C<u>H</u>).

^{19}F NMR (376 MHz, $CDCl_3$, δ ppm, Fig. S2): -71.5 (-C<u>F</u>$_3$, $^3J_{HF}$ = 6 Hz).

^{13}C NMR (100 MHz, $CDCl_3$, δ ppm, Fig. S3): 32.0 (–<u>C</u>H$_2$), 82.5 (-<u>C</u>H), 122.0 (–C<u>F</u>$_3$), 208 (–**C**=S).

2.2. RAFT homopolymerization of VDF in the presence of cy-XA. A typical homopolymerization of VDF was carried out in a 100 mL Hastelloy autoclave Parr system (HC 276) equipped with a manometer, a mechanical Hastelloy anchor, a rupture disk (3000 PSI), and inlet and outlet valves. An electronic device regulated and controlled both stirring and heating of the autoclave. Prior to reaction, the autoclave was pressurized with 30 bars of nitrogen for 1 h to check for leaks. Then, the autoclave was conditioned for the reaction with several nitrogen/vacuum cycles (10^{-2} mbar) to remove any trace of oxygen. It was then filled under vacuum with TAPE initiator (54 mg, 0.234 mmol), 5-(trifluoromethyl)-1,3-oxathiolane-2-thione, cy-XA chain transfer agent (440 mg, 2.34 mmol), and DMC as the solvent (60 mL). The vessel was cooled in an acetone/liquid nitrogen bath and 3 freeze-pump-thaw cycles were applied before the fluorinated gas, VDF (15.0 g, 234 mmol) was transferred into the autoclave under weight control. Then, after warming up to room temperature, the reactor was stirred and gradually heated up to 74 °C and the evolutions of pressure and temperature were recorded. The maximum pressure, P_{max}, reached 29 bar, while the final pressure recorded was 14 bar. After the reaction was stopped, the autoclave was cooled to room temperature, and then placed in an ice bath. The unreacted monomer was purged off, the solvent and unreacted cy-XA (if there was any) were completely removed under vacuum. The total product mixture was precipitated from chilled pentane, filtered off and then dried under vacuum (20×10^{-3} bar, 50 °C) for 16 h.

The yield of the polymerization was determined gravimetrically (mass of polymers obtained/mass of monomer transferred into the pressure reactor) (yield = 61%). The obtained homopolymer, as a light yellow color fine powder, was characterized by ^{1}H and ^{19}F NMR spectroscopy.

^{1}H NMR (400 MHz, acetone-d_6, δ ppm of entry P1, Table S1, Fig. S6): 0.85 (s, -CH_3 signal of the α-end group arising from TAPE fragment); 1.85 (1H, t, $^{3}J_{HF}$ = 12 Hz, -$CF_2C\underline{H}_2$-H); 2.20 to 2.30 (m, -CF_2CH_2-CH_2CF_2-$C\underline{H}_2CF_2$ adjacent to the reverse T-T VDF-VDF dyad addition), 2.30 to 2.60 (m, -$CF_2C\underline{H}_2$-$C\underline{H}_2CF_2$- reverse T-T VDF-VDF dyad addition) and {-[PVDF-S-(C=S)-$CH(CF_3)C\underline{H}_2$}]$_n$-$C\underline{H}_2CF_2$-$(VDF)_x$; 2.60 to 3.35 (m, -$C\underline{H}_2CF_2$-$C\underline{H}_2CF_2$-, normal H-T VDF-VDF dyad addition), 3.4 (m, 2H, {-[PVDF-S-(C=S)-$CH(CF_3)C\underline{H}_2$}]$_n$-CF_2CH_2-$(VDF)_x$); 4.25 ppm (t, 2H, $^{3}J_{HF}$ = 8 Hz, -CH_2CF_2-$CF_2C\underline{H}_2$-S-(C=S)-); 5.3 (m, 1H, -$C\underline{H}(CF_3)$ of PVDF-XA); small signals between 6.05 and 6.45 (tt, $^{2}J_{HF}$ = 55 Hz, $^{3}J_{HH}$ = 4.6 Hz, -CH_2CF_2-$\underline{H}$ end-group caused either by the transfer to the solvent or polymer or from the backbiting.[2]

^{19}F NMR (376 MHz, acetone-d_6, δ ppm of entry P1, Table S1, Fig. 1): -71.5 {-[PVDF-S-(C=S)-$CH(C\underline{F}_3)CH_2$]$_n$-}; -91.5 (-$CH_2C\underline{F}_2$-$CH_2C\underline{F}_2$-, normal VDF-VDF dyad addition); -95.1 (-CH_2CF_2-CH_2CF_2-CF_2CH_2-$CH_2C\underline{F}_2$-CH_2CF_2-, VDF adjacent to reverse VDF-VDF dyad addition); -107.4 ($C\underline{F}_2CH_2$-H); −112.2 (-$CH_2C\underline{F}_2$-CF_2CH_2-S), −113.2 (-$CH_2C\underline{F}_2$-CF_2CH_2−CH_2, reverse addition of VDF); -114.5 (dtt, $^{2}J_{HF}$ = 55 Hz, $^{3}J_{HF}$ = 16 Hz and $^{4}J_{FF}$ = 6 Hz, -CF_2-$CH_2C\underline{F}_2$-H, chain-end from transfer or back-biting); -114.8 (-CH_2CF_2-$C\underline{F}_2CH_2$-S); -115.8 (h_b, -CH_2CF_2-$C\underline{F}_2CH_2$−CH_2, reverse addition of VDF).

^{13}C NMR (100 MHz, acetone-d_6, δ ppm of entry P1, Table S1, Fig. S7): 23.1 (-$CF_2\underline{C}H_2$-$\underline{C}H_2CF_2$, VDF–VDF TT reverse addition); 37.15 [-$OCH(CF_3)\underline{C}H_2$ of XA]; 44.30 (-$\underline{C}H_2$ of VDF, $^{2}J_{CF}$ = 31 Hz); 55.00 [-CH_2CF_2-$CF_2\underline{C}H_2$-S-(C=S)-]; 71.50 [-$O\underline{C}H(CF_3)CH_2$ of XA]; 118.40 to 123.30 [q, -$OCH(\underline{C}F_3)CH_2$ of XA, $^{1}J_{CF}$ = 254 Hz]; 119.80 to 127.00 (*t*, -$\underline{C}F_2$ of VDF, $^{1}J_{CF}$ = 280 Hz); 129.70 [t, -CH_2CF_2- $CH_2\underline{C}F_2$-S(C=S)-, $^{1}J_{CF}$ = 314 Hz]; 206.70 (-$O\underline{C}$=S of XA).

2.3. Kinetics study of RAFT polymerization of VDF mediated by cy-XA. Aliquots were collected periodically from the autoclave in the course of the polymerization to monitor (i) the

conversion of VDF and (ii) the evolution of the molar masses *versus* time. The collected samples were frozen immediately in a liquid nitrogen bath and then were allowed to warm to room temperature to evaporate out the unreacted VDF. Subsequently, the samples were dried under vacuum for 2 h at room temperature and were characterized by means of SEC and NMR spectroscopy.

The VDF conversion (α_{VDF}) was determined by ^{19}F NMR spectroscopy using the following equation:

$$\alpha_{VDF} = \frac{(\int_{-91}^{-96} CF_2 \ + \int_{-106}^{-108} CF_2 \ + \int_{-113}^{-117} CF_2)/2}{\int_{-70}^{-72} CF_3 \ /3} \times \frac{[cy-XA]_0}{[VDF]_0} \qquad (S1)$$

where $\int_{-i}^{-j} CF_x$ stands for the integral of the signal assigned to CF_x ranging from -*i* ppm to -*j* ppm in the ^{19}F NMR spectrum.

The theoretical molar masses of the synthesized polymers were calculated using the following equation:

$$M_{n,theo.} = \{([\text{VDF}]_o/[\text{cy-XA}]_o) \times M_{VDF} \times \alpha_{VDF}\} + M_{cy\text{-}XA} \qquad (S2)$$

where M_{VDF} and $M_{cy\text{-}XA}$ stand for the molar masses of VDF (64 g mol^{-1}) and cyclic xanthate (188 g mol^{-1}).

Determination of Chain End Functionality. The chain end functionalities were determined using the following equations:

$$\%-CH_2CF_2XA\ functionality = \frac{\frac{1}{2}\int_{3.18}^{3.25} -CH_2CF_2XA}{\frac{1}{2}\int_{3.18}^{3.25} -CH_2CF_2XA + \frac{1}{2}\int_{4.17}^{4.26} -CF_2CH_2XA} \times 100 \qquad (S3)$$

$$\%-CF_2CH_2XA\ functionality = \frac{\frac{1}{2}\int_{4.17}^{4.26} -CF_2CH_2XA}{\frac{1}{2}\int_{3.18}^{3.25} -CH_2CF_2XA + \frac{1}{2}\int_{4.17}^{4.26} -CF_2CH_2XA} \times 100 \qquad (S4)$$

2.4. Cleavage of the polymer. The as-synthesized multiblock PVDF was cleaved following a procedure described earlier by Wang et al.[3] A solution of original polymer was treated with butylamine in THF at room temperature for 30 min and followed by precipitated into chilled pentane. It was then filtered off and dried under vacuum (20×10^{-3} bar, 50 °C) for 16 h to obtain light brownish powder with quantitative yield. PVDF-SH was characterized by ^{1}H and ^{19}F NMR spectroscopy (Fig. S8-S9).

^{1}H NMR (400 MHz, acetone-d_6, δ ppm Fig. S8): 0.85 (s, -CH_3 signal of the α-end group arising from TAPE fragment); 1.5 ppm (-CH_2-S$\underline{H}$[4]); 1.85 (1H, t, $^{3}J_{HF}$ = 12 Hz, -$CF_2C\underline{H}_2$-H); 2.20 to 2.30 (m, -CF_2CH_2-CH_2CF_2-$C\underline{H}_2CF_2$ adjacent to the reverse T-T VDF-VDF dyad addition), 2.30 to 2.60 (m, -$CF_2C\underline{H}_2$-$C\underline{H}_2CF_2$- reverse T-T VDF-VDF dyad addition); 2.60 to 3.20 (m, -$C\underline{H}_2CF_2$-$C\underline{H}_2CF_2$-$C\underline{H}_2CF_2$-, normal H-T VDF-VDF dyad addition); 3.3 (-$CF_2C\underline{H}_2$-SH, $^{3}J_{HF}$ = 16 Hz, $^{3}J_{HH}$ = 7 Hz); 6.70 to 6.95 ppm (olefinic protons resulting from the dehydrofluorination of PVDF in the presence of base[5-7]).

^{19}F NMR (376 MHz, acetone-d_6, δ ppm Fig. S9): -91.5 (normal VDF-VDF dyad addition, -$CH_2C\underline{F}_2$-$CH_2C\underline{F}_2$-);-95.1 (-CH_2CF_2-CH_2CF_2-CF_2CH_2-$CH_2C\underline{F}_2$-CH_2CF_2-, VDF linked to reverse VDF-VDF dyad addition); -107.4 ($C\underline{F}_2CH_2$-H); −112.2 (-$CH_2C\underline{F}_2$-CF_2CH_2-SH); −113.2 (-$CH_2C\underline{F}_2$-CF_2CH_2−CH_2, reverse addition of VDF); -114.5 (dtt, $^{2}J_{HF}$ = 55 Hz, $^{3}J_{HF}$ = 16 Hz and $^{4}J_{FF}$ = 6 Hz, -CF_2-$CH_2C\underline{F}_2$-H, chain-end from transfer); -115.8 (h_b, -CH_2CF_2-$C\underline{F}_2CH_2$−CH_2, reverse addition of VDF); -116.4 (-CH_2CF_2-$C\underline{F}_2CH_2$-S).

2.5. Synthesis of PVDF-*b*-PVAc multiblock copolymer using PVDF-XA as macroCTA. A typical synthesis of a PVDF-*b*-PVAc block copolymer was performed using Schlenk techniques under nitrogen atmosphere as follows (Scheme 1): PVDF-XA macroCTA (P1, Table S1) (0.49 g, 0.03 mmol) and V-70 (2 mg, 0.003 mol) were dissolved in 1.5 mL of DMF. The solution was

stirred and bubbled with N_2 for 20 min, and then degassed VAc (0.8 mL, 9 mmol) was added under a nitrogen flux and the reaction mixture was heated at 40 °C under stirring for 24 h. At the end of the reaction, the unreacted VAc was removed under vacuum. The crude product was then dissolved in acetone and precipitated twice from chilled pentane, filtered through a filter funnel, and then dried under vacuum (10^{-3} bar, 40 °C) for 16 h. The purified copolymer, as light yellow powder, was characterized by ^{1}H and ^{19}F NMR spectroscopy.

^{1}H NMR (400 MHz, acetone-d_6, δ ppm of P2, Table S1, Fig. S15): 1.90 ppm (-C$\underline{H}_2$ of VAc)[8]; 2.05 ppm (-OCOC$\underline{H}_3$ of VAc); 2.20 to 2.70 (m, -$CF_2C\underline{H}_2$-$C\underline{H}_2CF_2$- reverse T-T VDF-VDF dyad addition, overlapped with {-[PVDF-S-(C=S)-$C(CF_3)CH_2$}]$_n$-$C\underline{H}_2CF_2$-$(VDF)_x$); 2.55 to 3.35 (m, -$C\underline{H}_2CF_2$-$C\underline{H}_2CF_2$-, normal H-T VDF-VDF dyad addition), 3.4 (m, 2H, -C$\underline{H}_2$ of XA adjacent to CF_2 of PVDF in the next block); 4.1 {$^{3}J_{HH}$ = 8 Hz, 2H, -CH(OAc)C$\underline{H}_2$-S-(C=S)-}; 4.95 (-C$\underline{H}$OAc of VAc); 5.35 {1H, -C$\underline{H}_2$CH(OAc)-S-(C=S)-}; 5.55 (m, 1H, -C$\underline{H}$ of XA); 6.05 to 6.45 (tt, $^{2}J_{HF}$ = 55 Hz, $^{3}J_{HH}$ = 4.6 Hz, -CH_2CF_2-$\underline{H}$ end-group caused either by the transfer to the solvent or polymer or from the backbiting.[2]

^{19}F NMR (376 MHz, acetone-d_6, δ ppm of P2, Table S1, Fig. S16): -71.5 (-C$\underline{F}_3$ of XA); -91.5 (-$CH_2C\underline{F}_2$-$CH_2C\underline{F}_2$-, normal H-T VDF-VDF dyad addition); -95.1 (-CH_2CF_2-CH_2CF_2-CF_2CH_2-$CH_2C\underline{F}_2$-CH_2CF_2- normal VDF adjacent to reverse T-T VDF-VDF dyad addition); −113.9 (-$CH_2C\underline{F}_2$-CF_2CH_2−CH_2, reverse addition of VDF); -114.3 [-CH_2CF_2-C$\underline{F}_2CH_2$-CH_2CH(OAc)]; -115.2 (dtt, $^{2}J_{HF}$ = 55 Hz, $^{3}J_{HF}$ = 16 Hz and $^{4}J_{FF}$ = 6 Hz, -CF_2-$CH_2C\underline{F}_2$-H chain-end from transfer; -116.2 (−CH_2CF_2−C$\underline{F}_2CH_2$−CH_2, reverse addition of VDF).

^{13}C NMR (100 MHz, acetone-d_6, δ ppm of P2, Table S1, Fig. S17): 21.05 (-OCO$\underline{C}H_3$ of VAc); 33.00 {-O$\underline{C}$H(CF_3)CH_2 of XA}; 37.15 {-OCH(CF_3)$\underline{C}H_2$ of XA}; 39.50 (-$\underline{C}H_2$ of VAc); 44.35 (-$\underline{C}H_2$ of VDF); 54.80 {-CH_2CF_2-$CF_2\underline{C}H_2$-S-(C=S)-}; 67.65 (-$\underline{C}$HOAc of VAc); 118.10 to 123.10

{q, $^{1}J_{CF}$ = 244 Hz, -OCH(CF_3)CH_2 of XA}; 119.80 to 127.00 (t, $^{1}J_{CF}$ = 248 Hz, -CF_2 of VDF); 129.70 {-CH_2CF_2-CF_2CH_2-S-(C=S)-}; 170.51 (-OCOCH_3 of VAc); 206.70 {-O(C=S) of XA}.

2.6. Synthesis of PVDF-*b*-poly(VAc-*alt*-MAF-TBE) multiblock copolymer using PVDF-XA as macroCTA. The copolymerizations were carried out using Schlenk techniques under nitrogen atmosphere. A typical copolymerization (P3, Table S1) of VAc with MAF-TBE was performed as follows (Scheme 1): V-70 (2 mg, 0.006 mmol) was placed into a Schlenk flask which was then purged by three vacuum-nitrogen cycles. Then, degassed VAc (0.4 mL, 4.5 mmol) and MAF-TBE (0.8 mL, 4.5 mmol) were transferred under a nitrogen flux and the reaction mixture was heated at 40 °C under stirring for 15 h. At the end of the reaction, the unreacted monomers were removed under vacuum. The crude product was then dissolved in acetone and precipitated twice in chilled pentane, filtered through a filter funnel, and then dried under vacuum (10^{-3} bar, 40 °C) for 16 h. The purified copolymer was characterized by ^{1}H and ^{19}F NMR spectroscopy.

^{1}H NMR (400 MHz, acetone-d_6, δ ppm of P3, Table S1, Fig. S18): 1.50 {–C(CH_3)$_3$ of MAF-TBE}; 1.95 ppm ((-OCOCH_3 of VAc); 2.10 to 2.60 (m, -CF_2CH_2-CH_2CF_2- reverse T-T VDF-VDF dyad addition, overlapped with -CH_2 of VAc and MAF-TBE; 2.65 to 3.25 (m, -CH_2CF_2-CH_2CF_2, normal H-T VDF-VDF dyad addition), 3.35 (m, 2H, -CH_2 of XA); 5.25 (-CHOAc of VAc in the VAc-MAF-TBE alternating dyad); 5.55 (m, 1H, -CH of XA); 6.0 to 6.4 (tt, $^{2}J_{HF}$ = 55 Hz, $^{3}J_{HH}$ = 4.6 Hz, -CH_2CF_2-H end-group caused either by the transfer to the solvent or polymer or from the backbiting.[2]

^{19}F NMR (376 MHz, acetone-d_6, δ ppm of P3, Table S1, Fig. S19): -68.0 (-CF_3 of MAF-TBE in the copolymer); -71.5 (-CF_3 of XA); -91.5 (-CH_2CF_2-CH_2CF_2-, normal VDF-VDF dyad addition); -95.1 (-CH_2CF_2-CH_2CF_2-CF_2CH_2-CH_2CF_2-CH_2CF_2-, VDF unit adjacent to a reverse

VDF-VDF dyad addition); −113.9 (-$CH_2C\underline{F}_2$-CF_2CH_2−CH_2, reverse addition of VDF); -115.2 (dtt, $^2J_{HF}$ = 55 Hz, $^3J_{HF}$ = 16 Hz and $^4J_{FF}$ = 6 Hz, -CF_2-$CH_2C\underline{F}_2$-H, chain-end from transfer); -116.2 (-CH_2CF_2-$C\underline{F}_2CH_2$-CH_2, reverse addition of VDF).

^{13}C NMR (100 MHz, acetone-d_6, δ ppm of P3, Table S1, Fig. S20): 21.15 (-OCO$\underline{C}H_3$ of VAc); 27.90 {–C($\underline{C}H_3$)$_3$ of MAF-TBE}; 32.60 {-O$\underline{C}$H(CF_3)CH_2 of XA}; 37.00 {-OCH(CF_3)$\underline{C}H_2$ of XA}; 38.85 (-$\underline{C}H_2$ of VAc and MAF-TBE); 44.35 (-$\underline{C}H_2$ of VDF); 54.90 {–$\underline{C}$(CH_3)$_3$ of MAF-TBE}; 67.15 (-$\underline{C}$HOAc of VAc in the VAc-MAF-TBE alternating dyad); 84.10 {–$CH_2\underline{C}$(CF_3)CO_2C(CH_3)$_3$ of MAF-TBE}; 118.10 to 123.10 {-OCH($\underline{C}F_3$)CH_2 of XA, q, $^1J_{CF}$ = 250 Hz}; 119.00 to 129.00 –$\underline{C}F_3$ of MAF-TBE, t, $^1J_{CF}$ = 252 Hz; 119.80 to 127.00 -$\underline{C}F_2$ of VDF, t, $^1J_{CF}$ = 252 Hz; 123.50 to 130.00 {-CH_2CF_2-$\underline{C}F_2CH_2$-CH_2CH(-OCO$\underline{C}H_3$)-, t, $^1J_{CF}$ = 270 Hz }; 167.60 (-O$\underline{C}$OCH_3 of VAc); 170.20 (-$\underline{C}$OOC(CH_3)$_3$ of MAF-TBE); 206.80 {-O$\underline{C}$=S of XA}.

3- Characterization.

Nuclear Magnetic Resonance (NMR) Spectroscopy. The microstructures of the copolymers were determined by ^{1}H, ^{13}C and ^{19}F NMR spectroscopies, recorded on a Bruker AC 400 Spectrometer (400 MHz for ^{1}H and 376 MHz for ^{19}F). Coupling constants and chemical shifts are given in Hertz (Hz) and parts per million (ppm), respectively. The experimental conditions for recording ^{1}H [or ^{13}C or ^{19}F] NMR spectra were as follows: flip angle 90 ° [or 90 °or 30 °], acquisition time 4.5 s [or 0.3 s or 0.7 s], pulse delay 2 s [or 1 or 5 s], number of scans 32 [or 8192 or 64], and a pulse width of 12.5, 9.5 and 5.0 μs for ^{1}H, ^{13}C and ^{19}F NMR, respectively.

Size Exclusion Chromatography (SEC) Measurements. Molecular weights (M_ns) and dispersities ($Đ$s) of the (co)polymers were assessed from size exclusion chromatography (SEC)

with triple-detection GPC from Agilent Technologies using a PL0390-0605390 LC light scattering detector with two diffusion angles (15° and 90°), a PL0390-06034 capillary viscometer, and a 390-LC PL0390-0601 refractive index detector and two PL1113-6300 ResiPore 300 × 7.5 mm columns. DMF (containing 0.1 wt % of LiCl) was used as the eluent at a flow rate of 0.8 mL min^{-1} and toluene as the flow rate marker. The entire SEC-HPLC system was thermostated at 35 °C. Poly(methyl methacrylate) standards were used for calibrating the SEC instrument and the results were processed using the corresponding Agilent software.

MALDI-TOF spectrometry. MALDI-TOF mass spectra were carried out at Laboratoire de Mesures Physiques (Montpellier University) on a MALDI-TOF/TOF Bruker Ultraflex III time-of-flight mass spectrometer using a nitrogen laser for MALDI (λ = 337 nm). The measurements in positive ion were performed with a voltage and reflector lens potential of 25 and 26.3 kV, respectively. For negative ion mode, the measurements were done with ion source and reflector lens potential of 20 and 21.5 kV respectively. Mixtures of peptides were used for external calibration. The matrix and cationizing agent were trans-2-[3-(4-tertbutylphenyl)-2-methylprop-2-enylidene]malononitrile (DCTB, 10 mg mL^{-1} in $CHCl_3$) and NaI (10 mg mL^{-1} in methanol), respectively. The polymer concentration was 10 mg/mL in dimethylformamide (DMF). The polymer and matrix were mixed in a 4:10 volume ratio. NaI was first deposited on the target. After evaporation of solvent, the mixture, composed of polymer and matrix, was placed on the matrix-assisted laser desorption ionization (MALDI) target.

Thermogravimetric Analysis (TGA). The thermogravimetric analysis of the purified and dried polymer samples were performed under air using a TGA 51 apparatus from TA Instruments at a heating rate of 10 °C min^{-1} from room temperature to 580 °C.

Differential Scanning Calorimetry (DSC). DSC analyses of the (co)polymers were carried out using a Netzsch DSC 200 F3 instrument under N_2 atmosphere. The DSC instrument was calibrated with noble metals and checked before analysis with an indium sample (T_m = 156 °C). The heating or cooling range was from -40 °C to 170 °C at a scanning rate of 10 °C min^{-1}. After its insertion into the DSC apparatus, the sample was initially stabilized at 20 °C for 10 min. Then the first scan was made at a heating rate of 10 °C min^{-1} up to 170 °C. It was then cooled to 20 °C. Finally, a second scan was performed at a heating rate of 10 °C min^{-1} up to 170 °C. Melting points (T_ms) were evaluated from the second heating, taken at the maximum of the enthalpy peaks and its area determined the melting enthalpy (ΔH_m). This ensured elimination of the thermal history of the polymers during the first heating.

The degrees of crystallinity of the copolymers were determined using the following eqn:

$$Degree\ of\ crystallinity\ (\chi) = \frac{\Delta H_m}{\Delta H_c} \times 100 \qquad (S5)$$

where ΔH_c (104.5 J g^{-1}) and ΔH_m correspond to the enthalpy of melting of a 100% crystalline PVDF[9] and the heat of fusion of the copolymer (determined by DSC in J g^{-1}), respectively.

4- Supplementary tables.

Table S1. Experimental conditions and results for the RAFT synthesis of PVDF, PVDF-*b*-PVAc and PVDF-*b*-poly(VAc-*alt*-MAF-TBE) multiblock (co)polymers.[a]

entry	monomer	CTA	Initiator	solvent	Temp. (°C)	Time (°C)	Conv. (%)	Original[b]		Treated[c]		$T_{d10\%}$[d] (°C)	T_g[e] (°C)	T_m[e] (°C)	χ[e] (%)
								M_n	$Đ$	M_n	$Đ$				
P1	VDF	cy-XA	TAPE	DMC	74	24	61	16300	1.49	3900	1.26	382	n.o.[f]	168	45
P2	VAc	PVDF-XA (P1)	V-70	DMF	40	20	52	48400	1.68	16100	1.36	314	41	-	-
P3	VAc+ MAF-TBE	PVDF-XA (P1)	V-70	DMF	40	16	100	97600	1.51	36300	1.28	191	75	-	-

Acronyms: VDF: vinylidene fluoride; VAc: vinyl acetate; MAF-TBE: *tert*-butyl-2-trifluoromethacrylate TAPE: *tert*-amyl peroxy-2-ethylhexanoate; V-70: 2,2′-azobis (4-methoxy-2,4-dimethylvaleronitrile); DMC: dimethyl carbonate; DMF: N,N-dimthylformamide. [a]Conditions: Volume of solvent = 60 mL (for P1); Volume of solvent = 1.5 mL (for P2-P3);. [b]Molecular weights (M_n)s and dispersities ($Đ$) of the original PVD, determined by SEC in DMF. [c]Molecular weights (M_n)s and dispersities ($Đ$) of the cleaved PVDF after treatment with *n*-butylamine, determined by SEC in DMF. [d]Assessed by thermogravimetric analysis (TGA), under air at 10 °C min^{-1}. [e]Determined by differential scanning calorimetry (DSC); χ: crystallinity determined from eqn (S5). [f]Not observed by DSC.

For the multiblock PVDF, the degree of polymerization (DP_n) can be calculated from ^{19}F NMR spectrum:

$$DP_n\ of\ VDF = \frac{(\int_{-91}^{-96} CF_2\ + \int_{-106}^{-108} CF_2\ + \int_{-113}^{-117} CF_2\ ) \times 3}{\int_{-70}^{-72} CF_3 \times 2} = 29 \qquad (S6)$$

$$M_{n,(PVDF\text{-}XA)n,theo..} = \{(M_{VDF} \times DP_n) \times (\text{Number of PVDF block in the chain})\} + M_{cy\text{-}XA} \qquad (S7)$$

where M_{VDF} and $M_{cy\text{-}XA}$ stand for the molar masses of VDF (64 g mol^{-1}) and cy-XA (188 g mol^{-1}), respectively. $M_{n,(PVDF\text{-}XA)n,theo.}$ is given as $M_{n,theo.}$ in Table S2.

Table S2. Experimental conditions and results for the RAFT polymerization of VDF mediated by cy-XA at 74 °C vs. time[a] and molar masses (M_ns) and dispersity values ($Đs$) of treated PVDF-XA with n-$BuNH_2$.

Entry	Time (h)	Convn[b] (%)	$M_{n,theo.}$[c]	Original[d]		Treated[e]		-CF_2XA (%)	-CH_2XA (%)
				M_n	$Đ$	M_n	$Đ$		
1	1	8	700	3700	1.59	900	1.36	76	24
2	2	12	950	4400	1.50	1100	1.33	61	39
3	5	20	1500	5700	1.54	1400	1.31	43	57
4	9	31	2200	7900	1.51	1900	1.29	20	80
5	15	47	3200	12400	1.48	3000	1.28	7	93
6	24	61	4100	16300	1.49	3900	1.26	0	0

Acronyms: VDF: vinylidene fluoride; TAPE: *tert*-Amyl peroxy-2-ethylhexanoate; DMC: dimethyl carbonate. [a]Conditions: Volume of DMC = 60 mL. [b]Determined by gravimetry. [c]Calculated using eqn (S2). [d]M_ns and $Đ$s of the original PVDFs, determined by SEC in DMF. [e]M_ns and $Đ$s of the cleaved PVDF after treatment with *n*-butylamine, determined by SEC in DMF. [f]Assessed by ^{1}H NMR spectroscopy using eqn (S3). [g]Assessed by ^{1}H NMR spectroscopy using eqn (S4).

5- Supplementary figures.

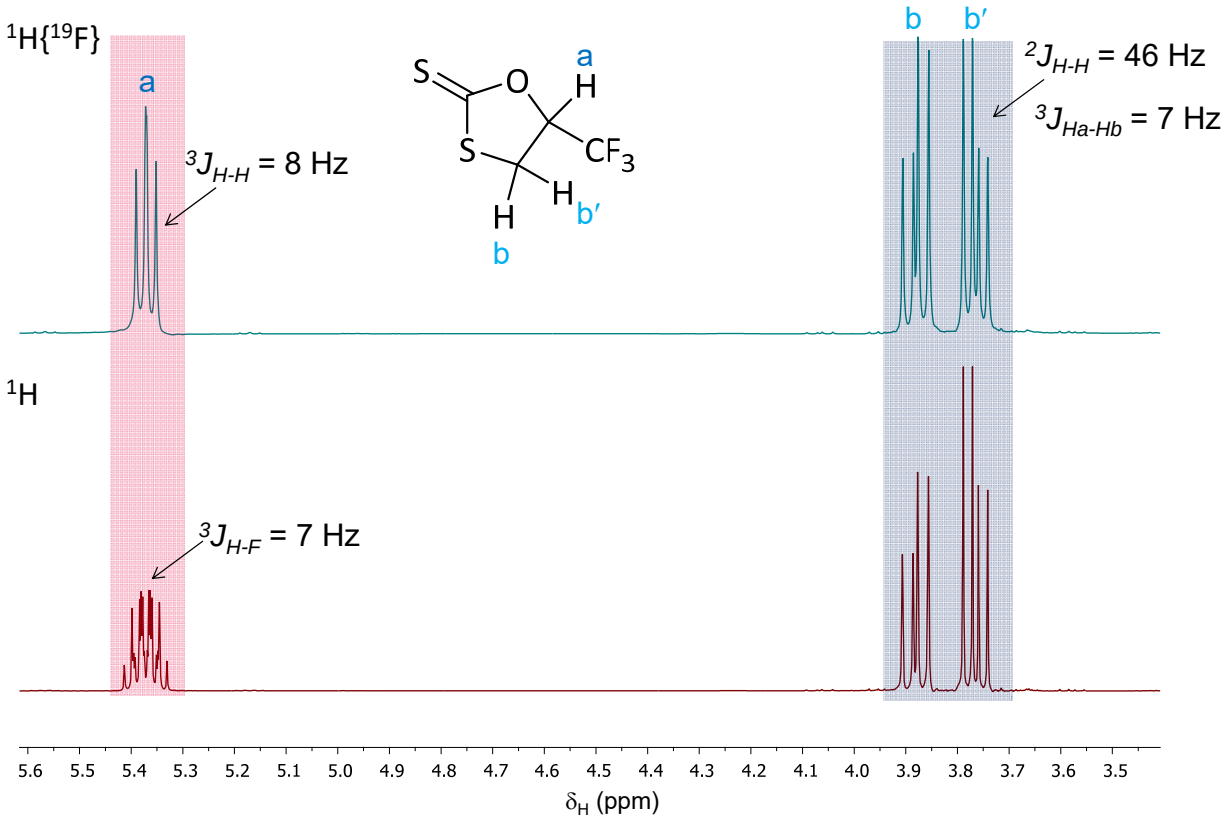

Fig. S1 Expansion of 3.4 to 5.6 ppm of the ^1H (non-decoupled, bottom) and $^1H\{^{19}F\}$ (^{19}F decoupled, top) NMR spectra of 5-(trifluoromethyl)-1,3-oxathiolane-2-thione (cy-XA), recorded in $CDCl_3$ at 20 °C.

The ^1H NMR spectrum of 5-(trifluoromethyl)-1,3-oxathiolane-2-thione (cy-XA) (Fig. S1) reveals two main signals characteristic of the -C<u>H</u>$_2$ and –C<u>H</u>,[1] centered at ca. 3.8 and 5.4 ppm, respectively. H_b and $H_{b'}$ protons are non-equivalent due to the presence of the asymmetric carbon atom bearing the –CF_3 group, and thus appear as a complex AB system centered at 3.8 ppm with $^2J_{HH}$ = 46 Hz. The H_a proton couples with the fluorine atoms in the -CF_3 group ($^3J_{H-F}$ = 7 Hz) and with H_b and $H_{b'}$. Comparison of the ^1H (non-decoupled, bottom) and $^1H\{^{19}F\}$ (^{19}F decoupled, top) NMR spectra confirms the structure of cy-XA. Indeed, in $^1H\{^{19}F\}$ (^{19}F decoupled, top) NMR spectrum, the H_a –F couplings are not observed. Instead, a characteristic triplet centered at 5.4 ppm was observed, displaying only H-H coupling ($^3J_{HH}$ = 8 Hz).

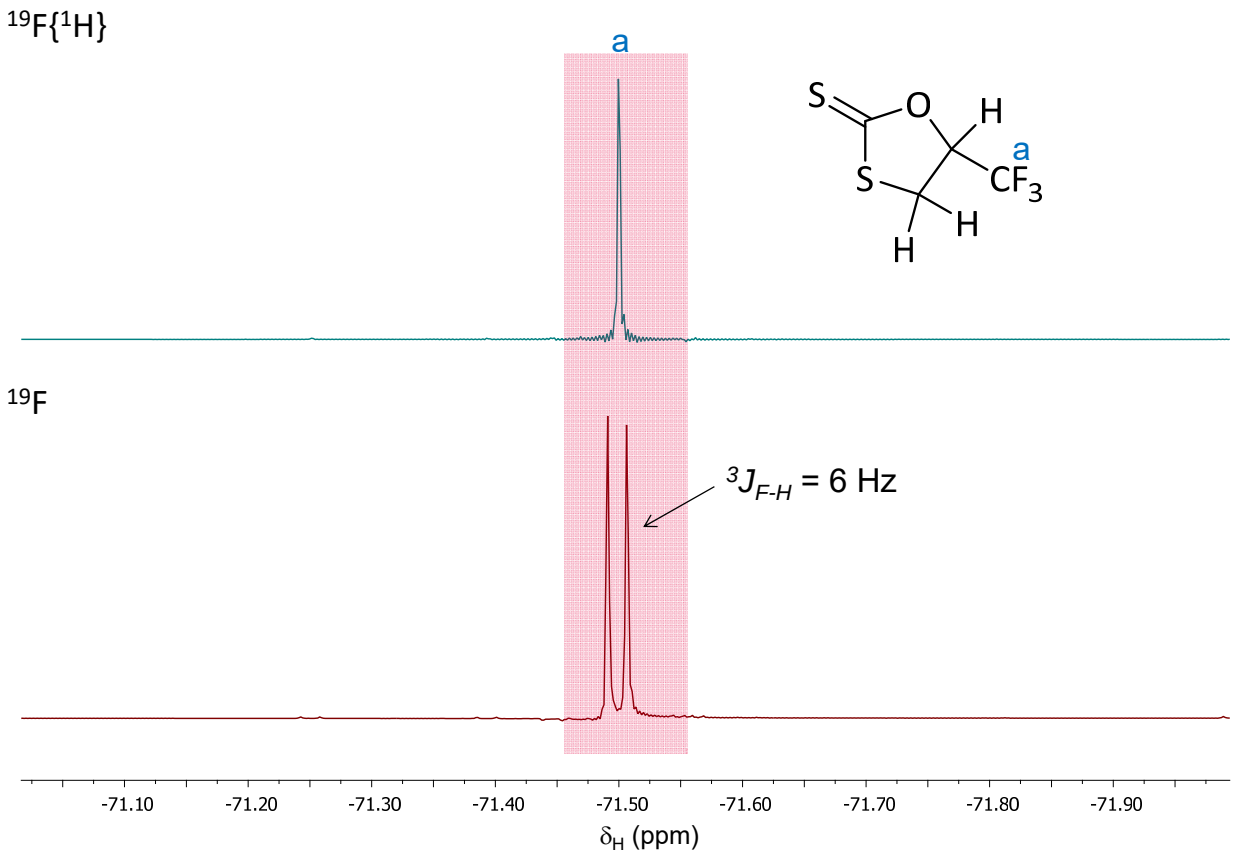

Fig. S2 Expansion of -71 to -72 ppm of the ^{19}F (non-decoupled, bottom) and $^{19}F\{^{1}H\}$ (^{1}H decoupled, top) NMR spectra of cy-XA, recorded in $CDCl_3$ at 20 °C.

The ^{19}F NMR spectrum of the cy-XA (Fig. S2) reveals the characteristic signal of the –C<u>F</u>$_3$ centered at ca. -71.5 ppm.[1] The F atoms couple with the adjacent H atom ($^{3}J_{F\text{-}H}$ = 6 Hz). The comparison of ^{19}F (non-decoupled, bottom) and $^{19}F\{^{1}H\}$ (^{1}H decoupled, top) NMR spectra confirms the structure of cy-XA. Indeed, in $^{19}F\{^{1}H\}$ (^{1}H decoupled, top) NMR spectrum the F-H couplings are not observed. Instead a characteristic singlet centered at -71.5 ppm was noticed.

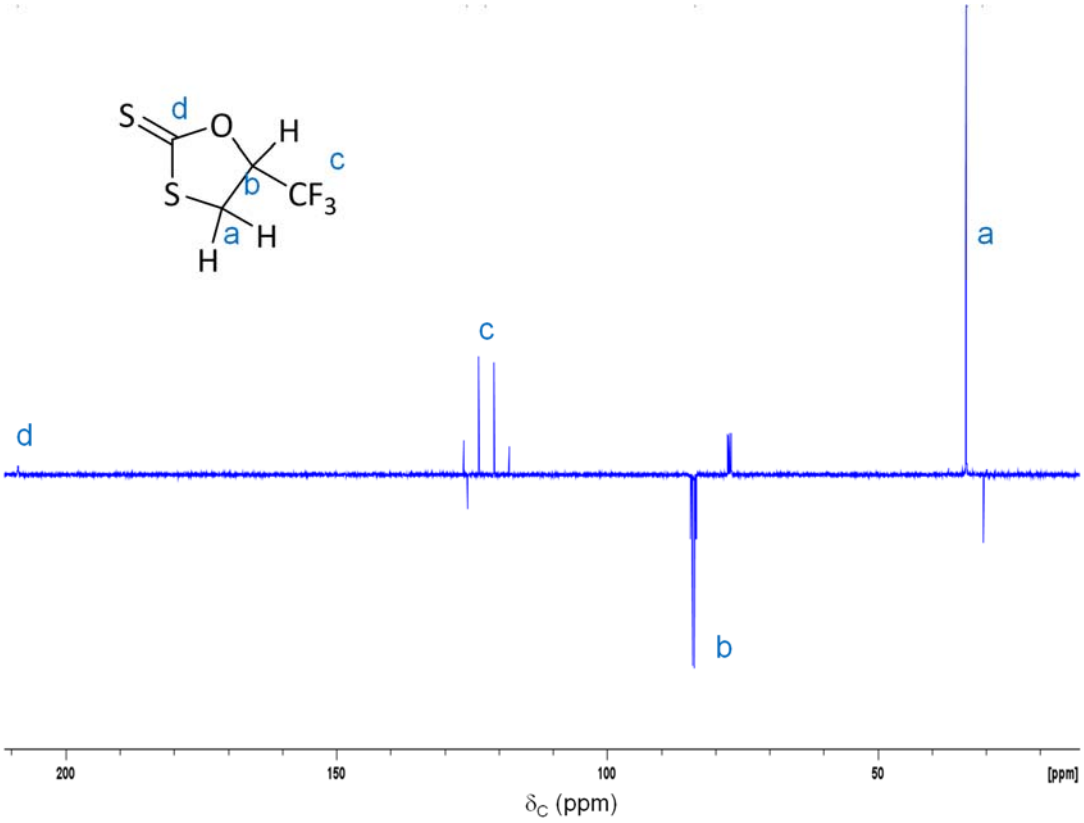

Fig. S3 ^{13}C NMR (C13APT) spectra of cy-XA, recorded in $CDCl_3$ at 20 °C.

The ^{13}C NMR (C13APT) spectrum of the cy-XA (Fig. S3) reveals the characteristic signals of the carbon atoms in –$\underline{C}H_2$, -$\underline{C}$H, –$C\underline{F}_3$ and –**C**=S groups centered at ca. 32.0, 82.5, 122 and 208 ppm, respectively.

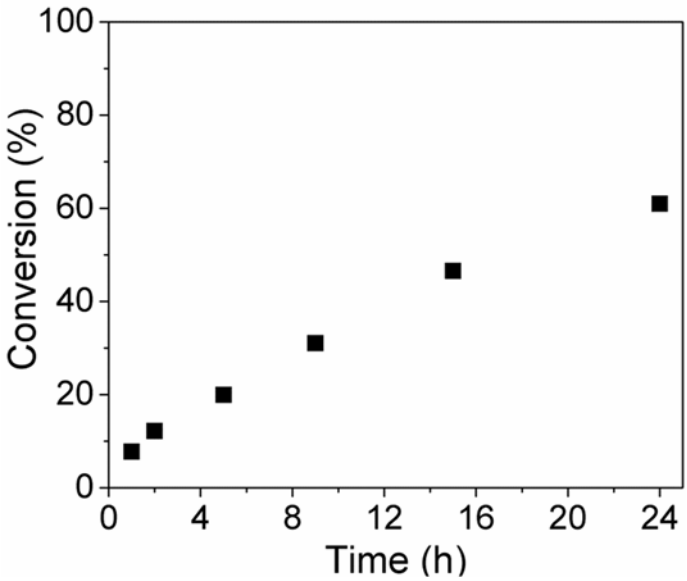

Fig. S4 VDF conversion vs. time plot for the RAFT polymerization of VDF mediated by 5-(trifluoromethyl)-1,3-oxathiolane-2-thione (cy-XA) at 74 °C in DMC.

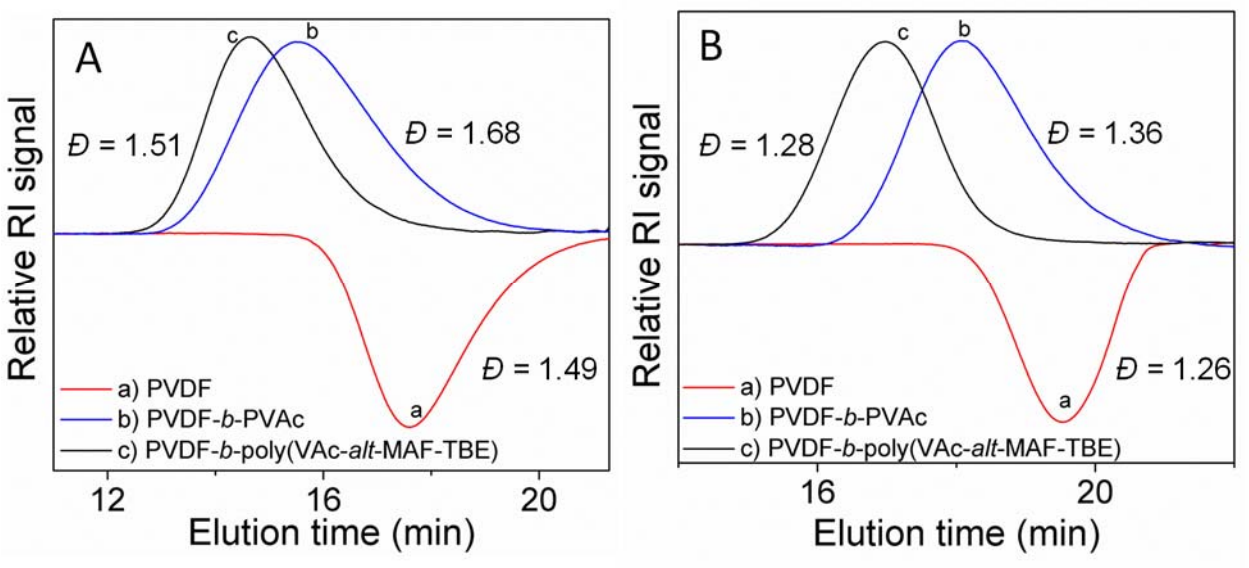

Fig. S5 SEC traces of (a) PVDF, (b) PVDF-*b*-PVAc and (c) PVDF-*b*-(VAc-*alt*-MAF-TBE) multiblock (co)polymers prepared thereof by RAFT (co)polymerization: (A) Original (co)polymers; (B) (Co)polymers treated with n-butylamine.

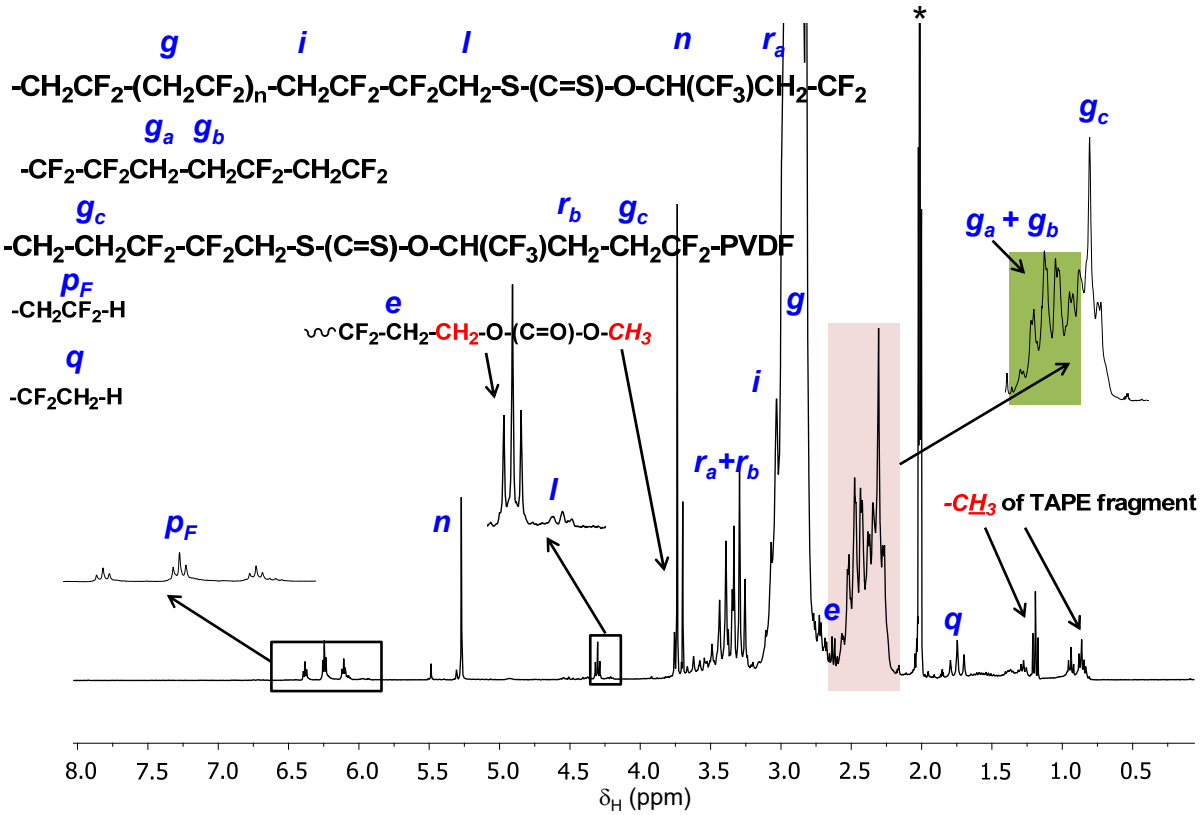

Fig. S6 Representative ^{1}H NMR spectrum of multiblock PVDF (P1, Table S1) prepared by RAFT polymerization of VDF mediated by cy-XA at 74 °C in DMC, recorded in acetone-d_6 at 20 °C. (*) Solvent (acetone) peak.

The ^{1}H NMR spectrum of the PVDF homopolymer (Fig. S6). reveals the characteristic signal of the -CF_2CH_2-CH_2CF_2-C$\underline{H}_2CF_2$ adjacent to the reverse T-T VDF-VDF dyad addition (m, 2.20 to 2.30 ppm), -$CF_2C\underline{H}_2$-C$\underline{H}_2CF_2$- reverse T-T VDF-VDF dyad addition (m, 2.35 to 2.60 ppm), -C$\underline{H}_2CF_2$-C$\underline{H}_2CF_2$-, normal H-T VDF-VDF dyad addition (m, 2.60 to 3.20 ppm), -C$\underline{H}_2$ and -C$\underline{H}$ of XA fragment (at 3.4 and 5.3 ppm, respectively), the triplet at 4.2 ppm ($^{3}J_{HF}$ = 8 Hz, -CH_2CF_2-$\underline{C}F_2CH_2$-S-(C=S)-) corresponding to the last VDF unit on the ω-chain-end (i.e., connected to the xanthate moiety), and a small triplet of triplets corresponding to the -CH_2CF_2-$\underline{H}$ end-group caused either by the transfer to the solvent or polymer or from the backbiting[2] (in the range of 6.05 to 6.45 ppm, $^{2}J_{HF}$ = 55 Hz, $^{3}J_{HH}$ = 4.6 Hz). These H-H additions are followed by irreversible trapping at the chain end by transfer to the XA (thus leading to {-$CF_2C\underline{H}_2$-S-(C=S)-C(C$\underline{F}_3$)CH_2}$_n$-$(CH_2CF_2)_x$}, but they can also propagate to add another unit of VDF in a tail-to-tail (TT) fashion. These additions can be easily identified as intrachain T-T defects by ^{1}H NMR (signals g_a and g_b, Fig. S6) and H-H defects by ^{19}F NMR (signals h_a, h_b, h_c and h_d, Fig. 1). -$CF_2C\underline{H}_2$• radicals formed via H-H addition can also transfer (to a much lesser extent than the transfer to the XA or propagation to another VDF unit) to the solvent (DMC) leading to -$CF_2C\underline{H}_2$-H dead chains. Such dead chains can be seen in Fig. S6 (signal *(q)* weak triplet at 1.85 ppm,[10] $CF_2C\underline{H}_2$-H and as a weak triplet at -107.4 ppm, $C\underline{F}_2CH_2$-H in the ^{19}F NMR spectrum, Fig. 1).[11] The characteristic signal for the normal H-T VDF-VDF addition was observed at -91.5 ppm (signal *h*) in the ^{19}F NMR spectrum (Fig. 1), while the –CF_3 corresponding to XA appears at -71.5 ppm.

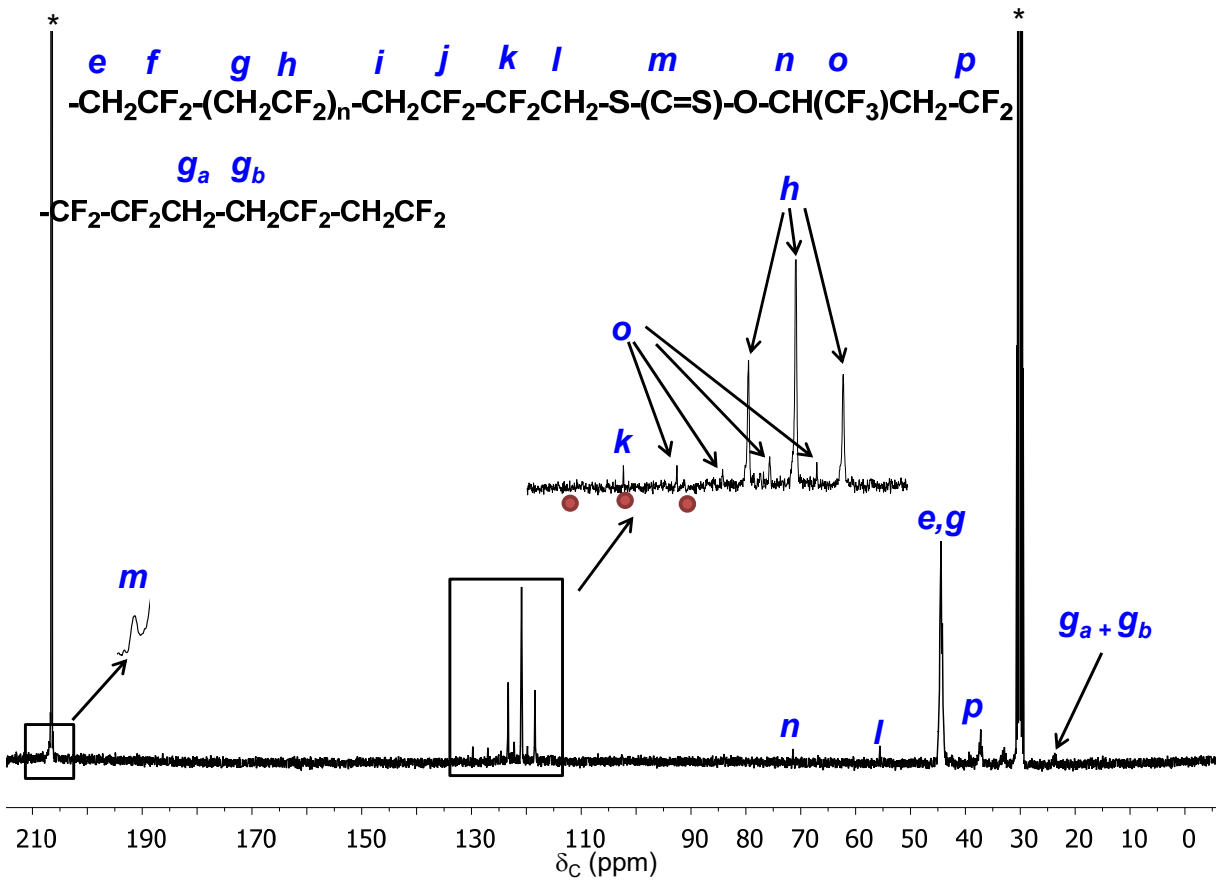

Fig. S7 Representative ^{13}C NMR spectrum of multiblock PVDF (entry P1, Table S1) prepared by RAFT polymerization of VDF mediated by cy-XA at 74 °C in DMC, recorded in acetone-*d*$_6$ at 20 °C. (*) Solvent (acetone) peak.

The ^{13}C NMR spectrum of the PVDF homopolymer (Fig. S7) exhibits the characteristic signals at 23.10 ppm (-$CF_2$$\underline{C}H_2$-$\underline{C}H_2CF_2$, VDF–VDF TT reverse addition)[10]; 37.15 ppm {-OCH(CF_3)$\underline{C}H_2$ of PVDF-XA}; 44.30 ppm (-$\underline{C}H_2$ of VDF); 55.00 ppm {-CH_2CF_2-$\underline{C}F_2\underline{C}H_2$-S-(C=S)}; 71.50 ppm {-O$\underline{C}$H($CF_3$)$CH_2$ of XA; 118.40 to 123.30 ppm {-OCH($\underline{C}F_3$)CH_2 of XA}; 119.80 to 127.00 ppm -$\underline{C}F_2$ of VDF; 129.70 ppm {-CH_2CF_2-$\underline{C}F_2CH_2$-S-(C=S)-}; 206.70 ppm {-O$\underline{C}$=S of XA}.

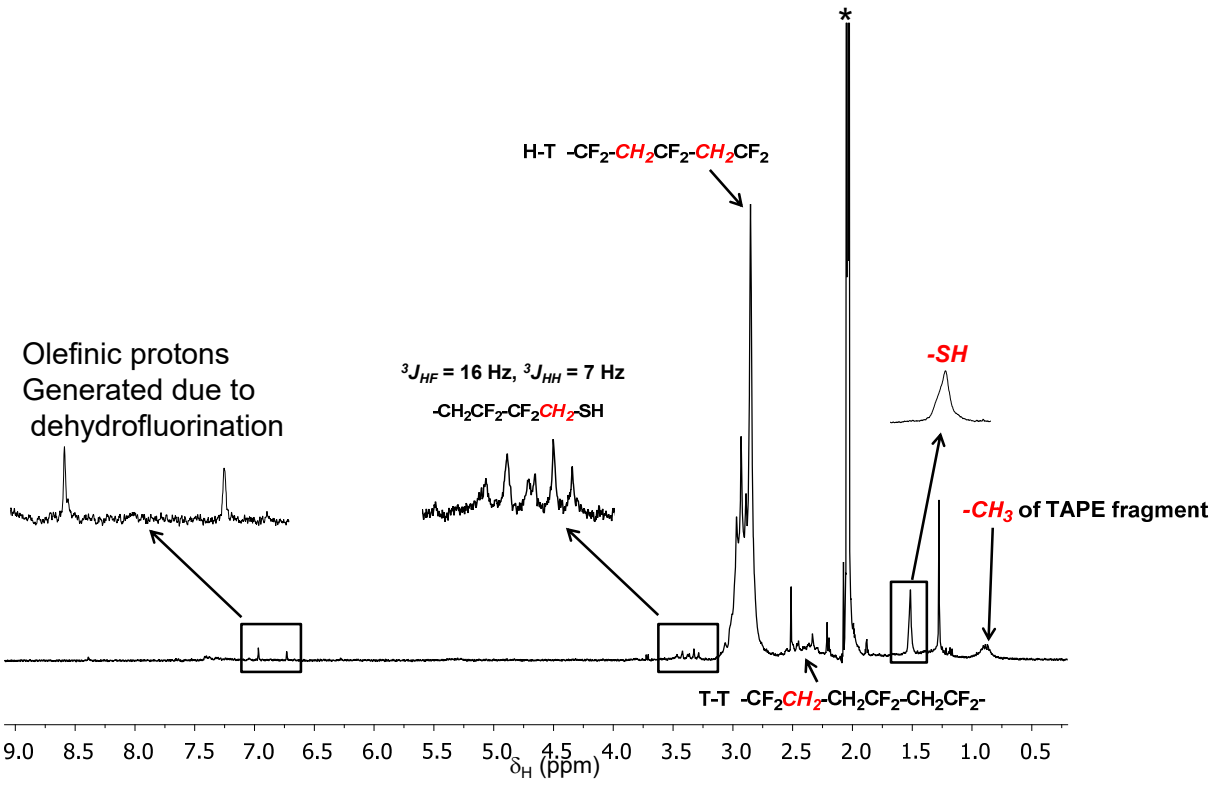

Fig. S8 Representative ^{1}H NMR spectrum of PVDF-SH prepared by n-butylamine treatment of multiblock PVDF (entry P1, Table S1), recorded in acetone-*d*$_6$ at 20 °C. (*) Solvent (acetone) peak.

After n-butylamine treatment and purification, the ^{1}H NMR spectrum of the PVDF-SH (Fig. S8) shows the elimination of the XA moiety (complete disappearance of the -CH$_2$ and -CH signals of XA (Z moieties) centered at 3.4 and 5.3 ppm, respectively) and the formation of the thiol end-group revealed by the appearance of a doublet of triplets at 3.3 ppm (with coupling constants $^{3}J_{HF}$ = 16 Hz, $^{3}J_{HH}$ = 7 Hz) in agreement with a -C<u>H</u>$_2$-SH moiety and also a singlet at 1.5 ppm assigned to the -S<u>H</u>.[4] Additionally, small signals appeared corresponding to the olefinic protons at 6.70 and 6.95 ppm. The origin of these olefinic protons is a well-documented dehydrofluorination of PVDF in the presence of base.[5-7]

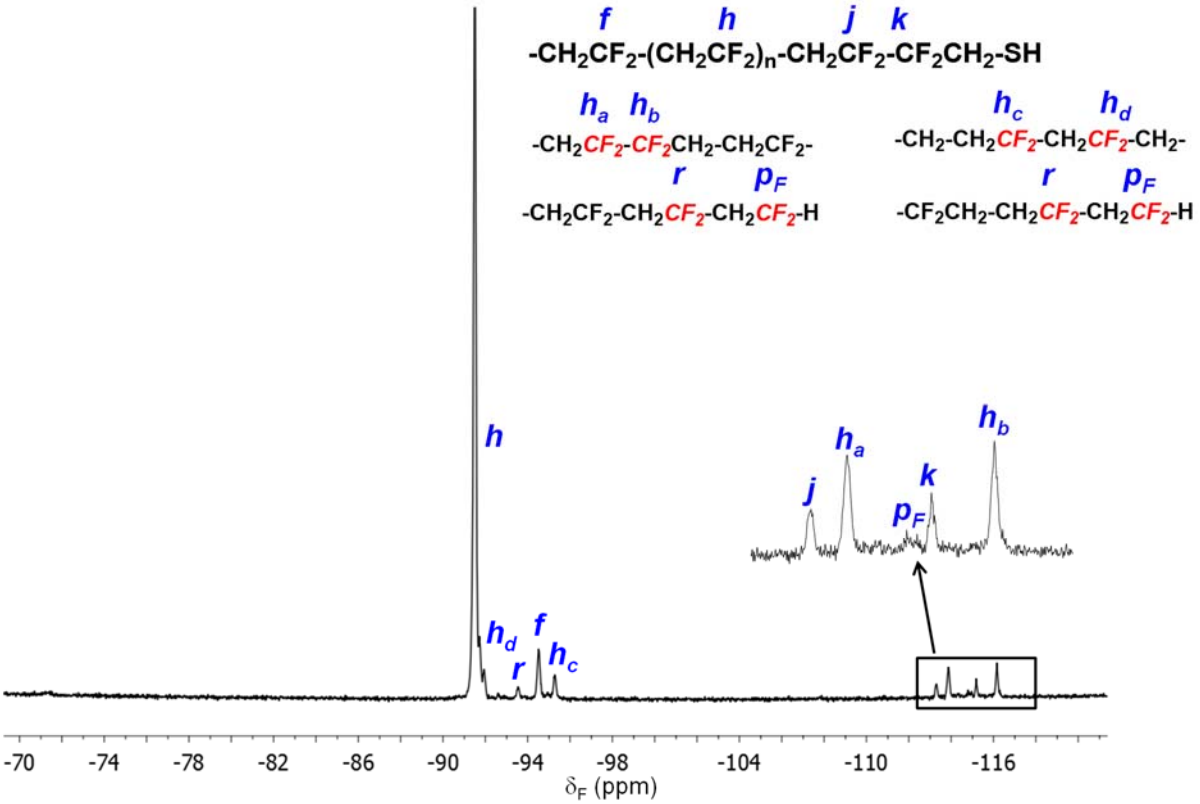

Fig. S9 Representative ^{19}F NMR spectrum of PVDF-SH prepared by n-butylamine treatment of multiblock PVDF (entry P1, Table S1), recorded in acetone-*d*$_6$ at 20 °C.

After n-butylamine treatment, the ^{19}F NMR spectrum of the PVDF-SH (Fig. S9) shows a surprising low field shift of the signal assigned to the C$\underline{F}_2$CH$_2$-XA (terminal VDF unit connected to XA) from -114.8 ppm to -116.4, suggesting the formation of C$\underline{F}_2$CH$_2$-SH.

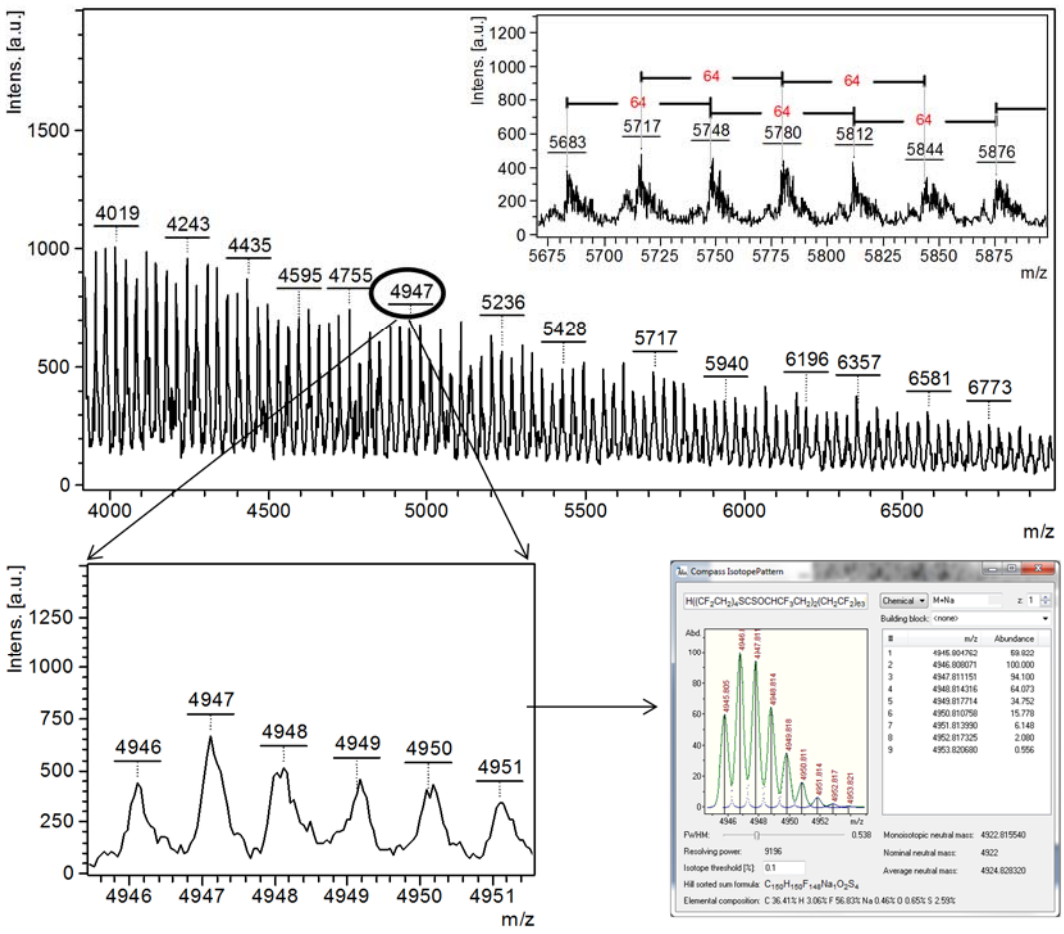

Experimental and theorical isotope pattern at 4947 *m/z* of $H(CF_2CH_2)_4SCSOCHCF_3CH_2)_2(CF_2CH_2)_{63}H$ sodium adduct

Fig. S10 Experimental and theoretical isotope pattern of m/z = 4947 of $H(CF_2CH_2)_4CSOCHCF_3(CF_2CH_2)_{63}H$.

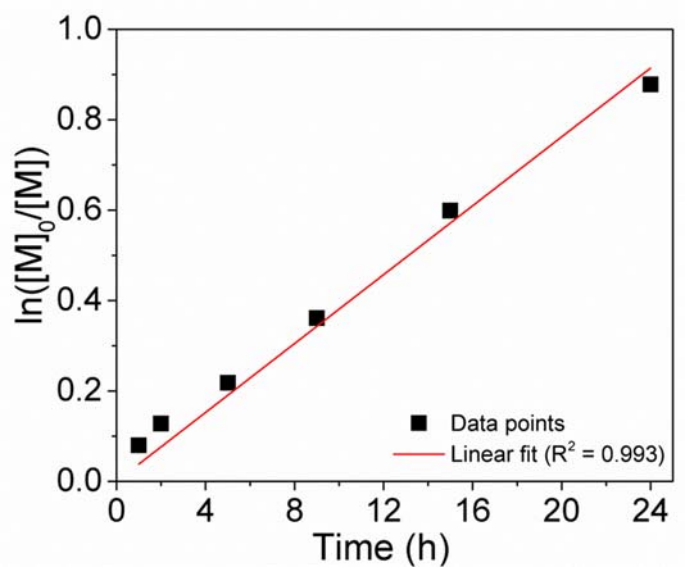

Fig. S11 ln[M]$_0$/[M] vs. time plot for the RAFT polymerization of VDF mediated by cy-XA at 74 °C in DMC.

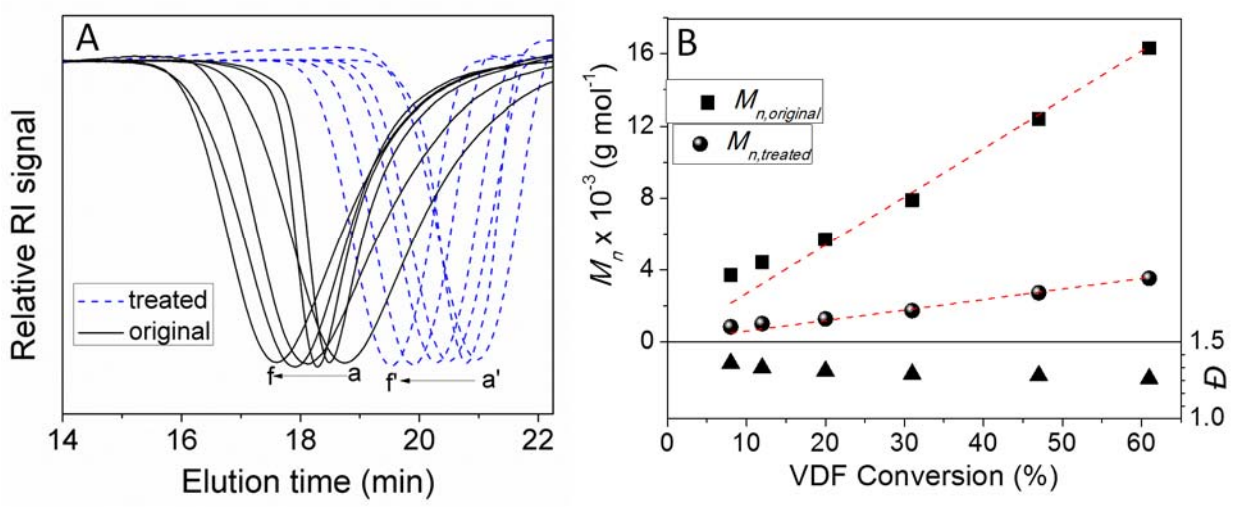

Fig. S12 A) Evolutions of the SEC traces of original (solid curves, a-f) and treated with $nBuNH_2$ (dotted curves, a′-f′) PVDFs (P1-P6, Table S2) and B) plot of M_ns and $Đ$s of original and treated PVDF vs. VDF conversion for the RAFT polymerization of VDF mediated by cy-XA.

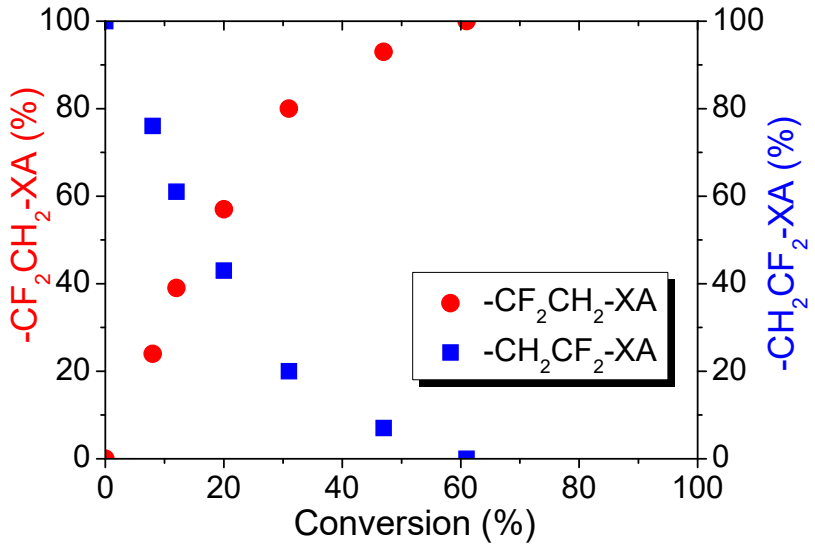

Fig. S13 Evolution of the chain-end functionalities for the RAFT polymerization of VDF mediated by cy-XA at 74 °C in DMC.

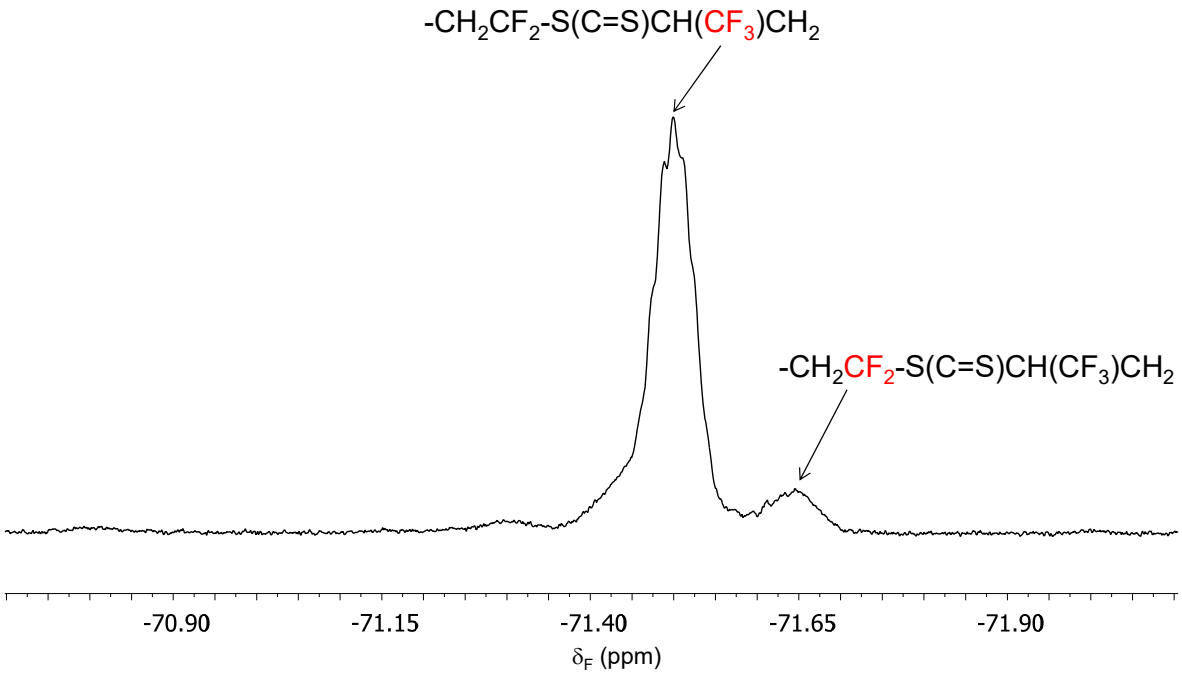

Fig. S14 Expansion of ^{19}F NMR spectrum of multiblock PVDF prepared by RAFT polymerization of VDF mediated by cy-XA at 74 °C in DMC (entry P1, Table S2, convn = 8%), recorded in acetone-d_6 at 20 °C.

The ^{19}F NMR spectrum of the multiblock PVDF at low conversion exhibited the characteristic peak for PVDF-CH_2CF_2-XA end-group.[12]

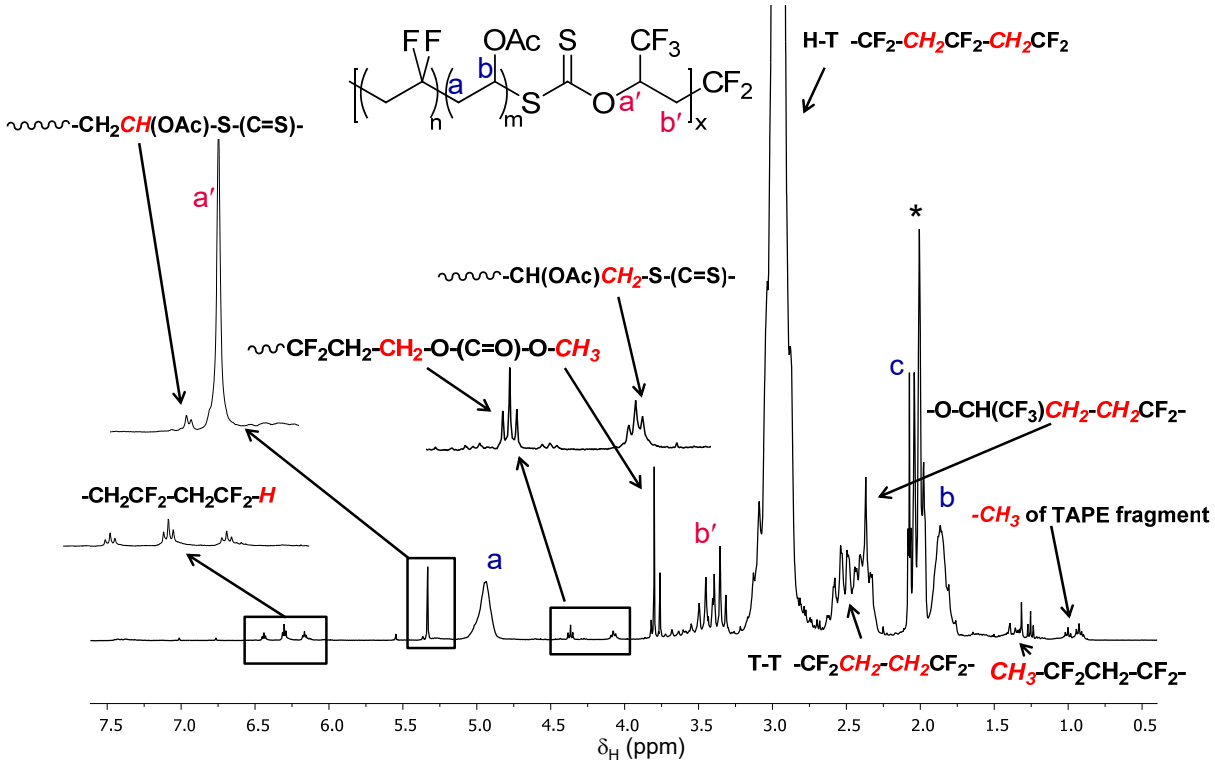

Fig. S15 ^{1}H NMR spectrum of PVDF-*b*-PVAc multiblock copolymer (entry P2, Table S1) prepared by RAFT polymerization, recorded in acetone-d_6 at 20 °C. (*) Solvent (acetone) peak.

The ^{1}H NMR spectrum of the PVDF-*b*-PVAc copolymer (Fig. S15). reveals three main signals characteristic of the (i) XA: -C<u>H</u>$_2$ and –C<u>H</u> (at 3.4 and 5.5 ppm, respectively); (ii) VDF: -CF$_2$C<u>H</u>$_2$-C<u>H</u>$_2$CF$_2$- reverse T-T VDF-VDF dyad addition, overlapped with -CH$_2$ of VAc (m, 2.20 to 2.70 ppm), -C<u>H</u>$_2$CF$_2$-C<u>H</u>$_2$CF$_2$-, normal H-T VDF-VDF dyad addition (m, 2.55 to 3.35 ppm), - and a small triplet of triplets corresponding to the -CH$_2$CF$_2$-<u>H</u> end-group caused either by the transfer to the solvent or polymer or from the backbiting[2] (in the range of 6.05 to 6.45 ppm, $^{2}J_{HF}$ = 55 Hz, $^{3}J_{HH}$ = 4.6 Hz) and (iii) VAc: -CH$_2$ of VAc (at 1.80-1.90 ppm), OCOC<u>H</u>$_3$ of VAc (2.05) and – CH(OAc)C<u>H</u>$_2$-S (corresponding to methylene in VAc unit adjacent to the ω-chain-end (i.e., connected to the xanthate moiety)[13-15] (4.1, t, $^{3}J_{HF}$ = 8 Hz)), C<u>H</u>OAc of VAc (4.95 ppm) and – CH$_2$C<u>H</u>(OAc)-S[8] (corresponding to the CH in VAc unit attached to the ω-chain-end (i.e., connected to the O-fluoroalkyl xanthate moiety) (5.35, m), while the signal assigned to C<u>H</u>(CF$_3$) appears at 5.32 ppm.

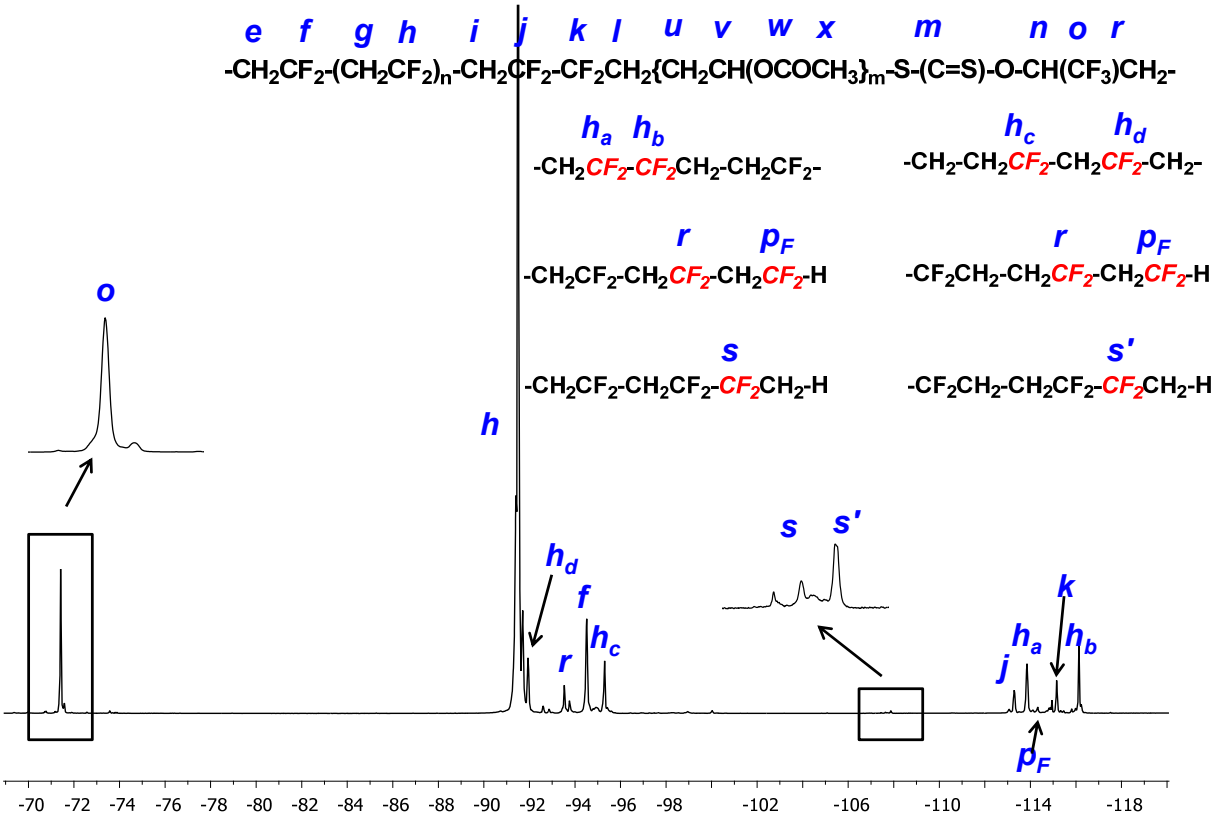

Fig. S16 ^{19}F NMR spectrum of PVDF-*b*-PVAc multiblock copolymer (entry P2, Table S1) prepared by RAFT polymerization, recorded in acetone-d_6 at 20 °C.

The ^{19}F NMR spectrum of the PVDF-*b*-PVAc copolymer (Fig. S16). reveals two main signals characteristic of the (i) XA: (-C$\underline{F}_3$ (-71.5 ppm) and (ii) VDF(-CH$_2$C$\underline{F}_2$-CH$_2$C$\underline{F}_2$-, normal VDF-VDF dyad addition (-91.5 ppm); (-CH$_2$CF$_2$-CH$_2$CF$_2$-CF$_2$CH$_2$-CH$_2$C$\underline{F}_2$-CH$_2$CF$_2$-; reverse VDF-VDF dyad addition (-95.1 ppm); -CH$_2$C$\underline{F}_2$-CF$_2$CH$_2$-CH$_2$ reverse addition of VDF (−113.9 ppm); -CH$_2$CF$_2$-C$\underline{F}_2$CH$_2$-CH$_2$CH(OAc) (-115.2 ppm, dtt, $^2J_{HF}$ = 55 Hz, $^3J_{HF}$ = 16 Hz and $^4J_{FF}$ = 6 Hz) -CF$_2$-CH$_2$C$\underline{F}_2$-H (-114.3 ppm) chain-end from transfer; −CH$_2$CF$_2$−C$\underline{F}_2$CH$_2$−CH$_2$, reverse addition of VDF (-116.2 ppm).

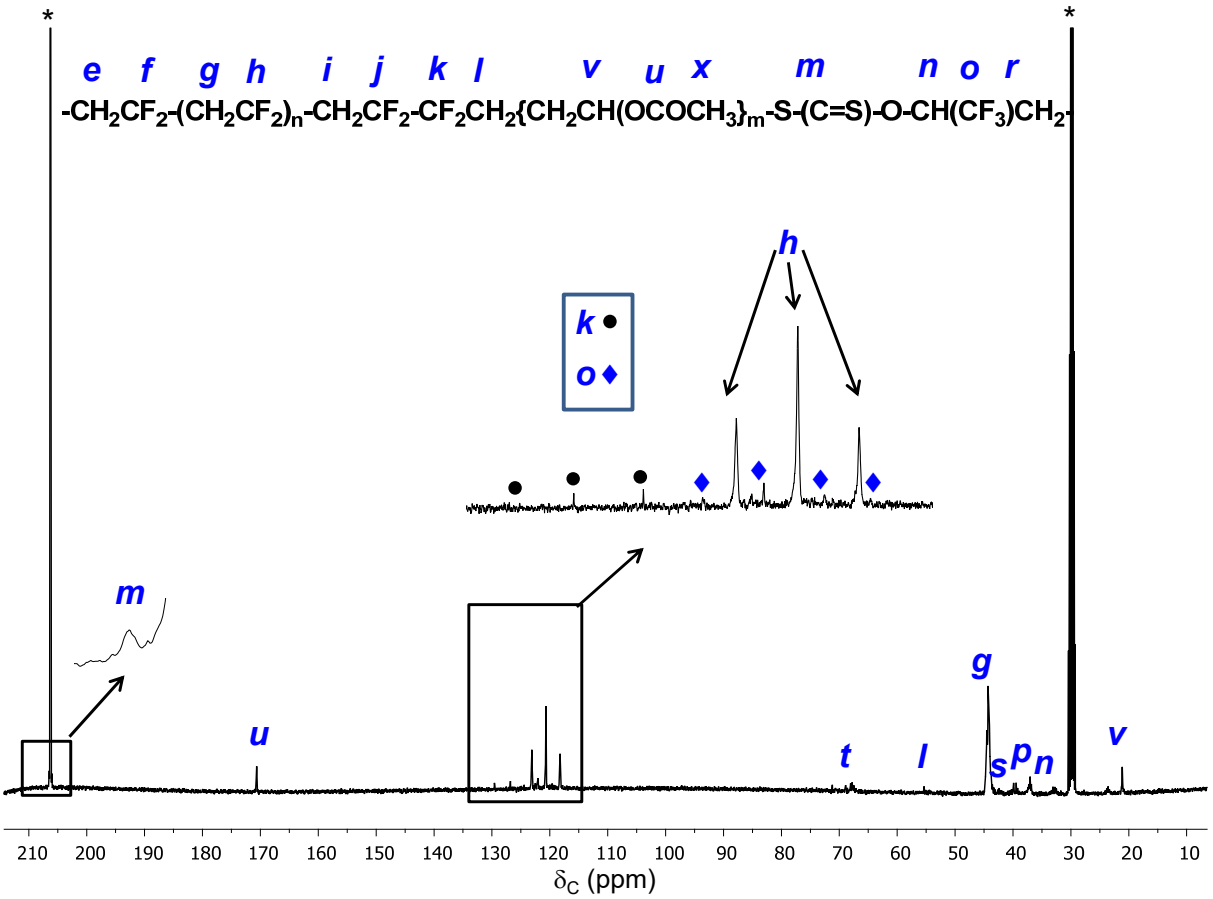

Fig. S17 ^{13}C NMR spectrum of PVDF-*b*-PVAc multiblock copolymer (entry P2, Table S1) prepared by RAFT polymerization, recorded in acetone-d_6 at 20 °C. (*) Solvent (acetone) peak.

The ^{13}C NMR spectrum of the PVDF-*b*-PVAc copolymer (Fig. S17) helps to confirm the structure. It exhibits the characteristic signals at 21.05 (-OCO$\underline{C}$H$_3$ of VAc); 33.00 {-O$\underline{C}$H(CF$_3$)CH$_2$ of XA}; 37.15 {-OCH(CF$_3$)$\underline{C}$H$_2$ of XA}; 39.50 (-$\underline{C}$H$_2$ of VAc); 44.35 (-$\underline{C}$H$_2$ of VDF); 54.80 {-CH$_2$CF$_2$-$\underline{C}$F$_2$CH$_2$-S-(C=S)-}; 67.65 (-$\underline{C}$HOAc of VAc); 118.10 to 123.10 {-OCH($\underline{C}$F$_3$)CH$_2$ of XA}; 119.80 to 127.00 -$\underline{C}$F$_2$ of VDF; 129.70 {-CH$_2$CF$_2$-$\underline{C}$F$_2$CH$_2$-S-(C=S)-}; 170.51 (-O$\underline{C}$OCH$_3$ of VAc); 206.70 {-O($\underline{C}$=S) of XA}.

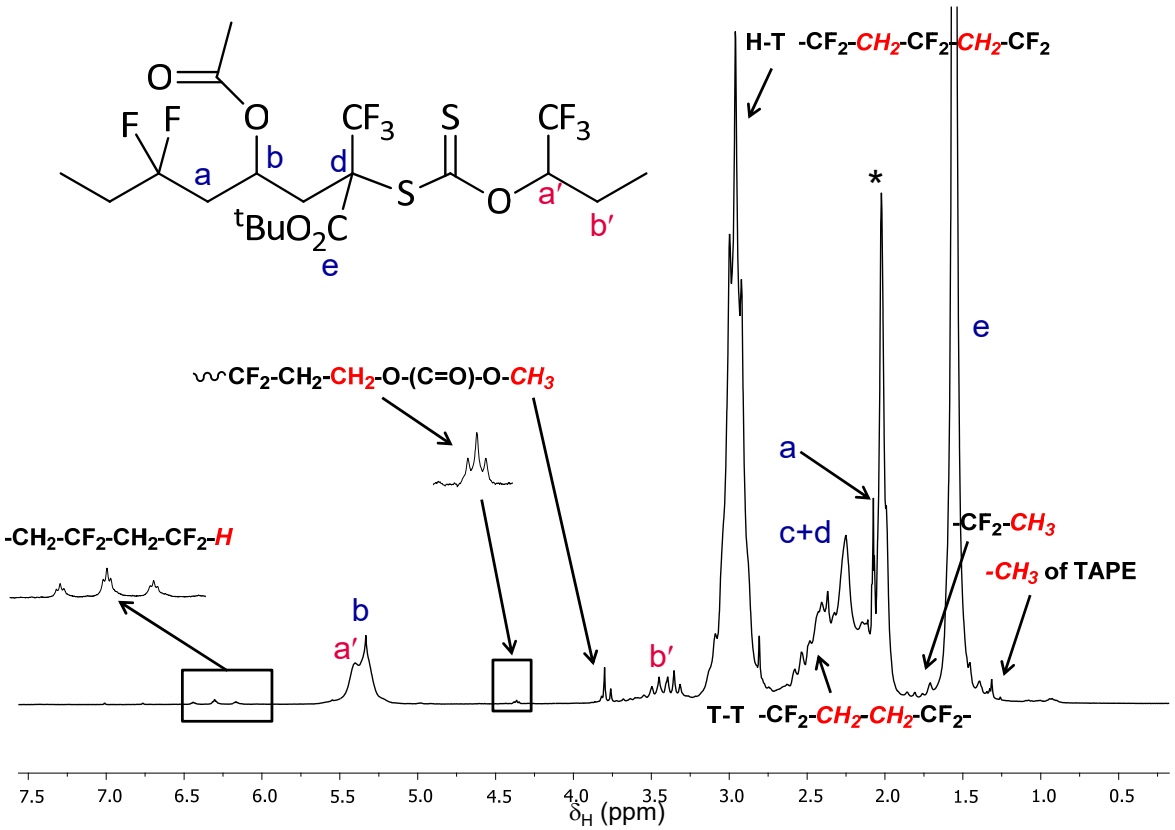

Fig. S18 ^{1}H NMR spectrum of PVDF-*b*-poly(VAc-*alt*-MAF-TBE) (entry P3, Table S1) prepared by RAFT polymerization, recorded in acetone-d_6 at 20 °C. (*) Solvent (acetone) peak.

The ^{1}H NMR spectrum of the PVDF-*b*-poly(VAc-*alt*-MAF-TBE) copolymer (Fig. S18) reveals three main signals characteristic of the (i) XA: -C$\underline{H}_2$ and –C$\underline{H}$ (at 3.35 and 5.55 ppm, respectively); (ii) VDF: -CF$_2$C$\underline{H}_2$-C$\underline{H}_2$CF$_2$- reverse T-T VDF-VDF dyad addition, overlapped with -CH$_2$ of VAc and MAF-TBE (m, 2.10 to 2.60 ppm), -C$\underline{H}_2$CF$_2$-C$\underline{H}_2$CF$_2$-, normal H-T VDF-VDF dyad addition (m, 2.65 to 3.25 ppm), and a small triplet of triplets corresponding to the -CH$_2$CF$_2$-$\underline{H}$ end-group caused either by the transfer to the solvent or polymer or from the backbitings[2] (in the range of 6.05 to 6.45 ppm, $^{2}J_{HF}$ = 55 Hz, $^{3}J_{HH}$ = 4.6 Hz); (iii) VAc: -CH$_2$ of VAc (at 1.90 ppm), -OCOC$\underline{H}_3$ of VAc (at 2.05 ppm),[13-15] and -C$\underline{H}$OAc of VAc (5.25 ppm) and (iv) MAF-TBE: -C(C$\underline{H}_3$)$_3$ of MAF-TBE (1.50) and -CH$_2$ of MAF-TBE, overlapped with -CF$_2$C$\underline{H}_2$-C$\underline{H}_2$CF$_2$- reverse T-T VDF-VDF dyad addition and -CH$_2$ of VAc (2.10 to 2.60).

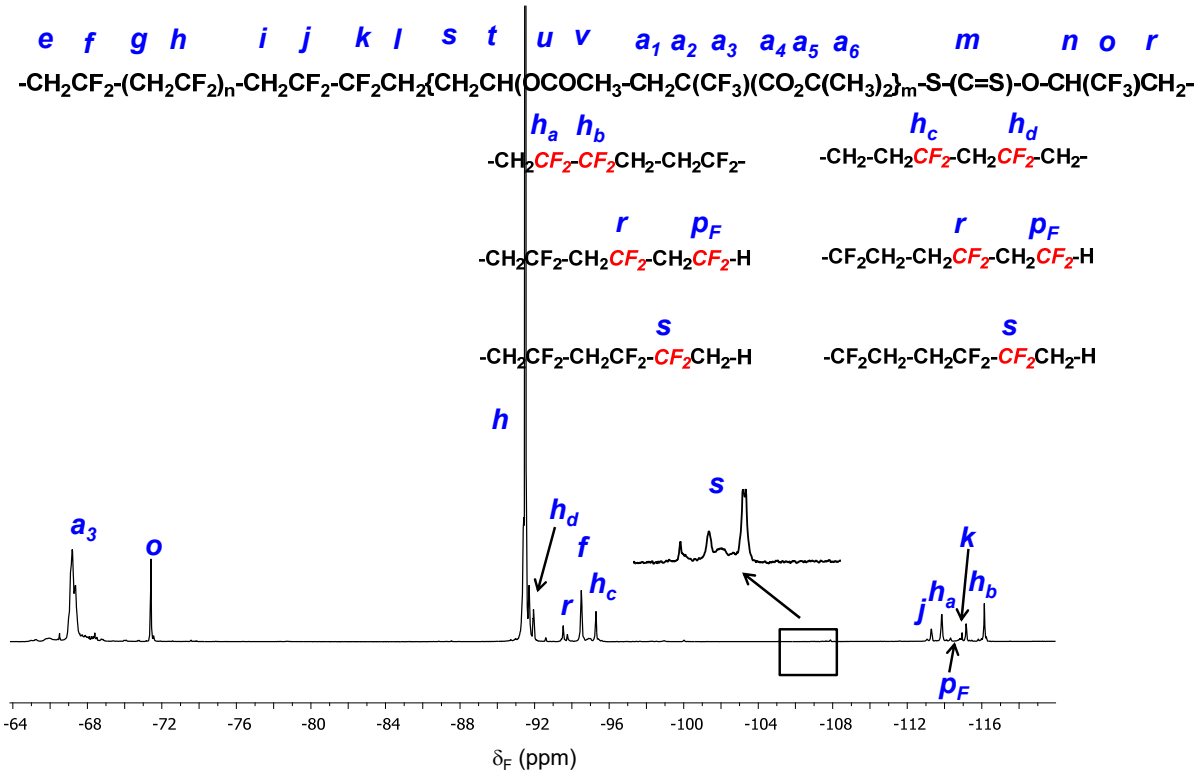

Fig. S19 ^{19}F NMR spectrum of PVDF-*b*-poly(VAc-*alt*-MAF-TBE) (entry P3, Table 1) prepared by RAFT copolymerization of VAc with MAF-TBE in the presence of PVDF-XA macroRAFT agent, recorded in acetone-d_6 at 20 °C.

The ^{19}F NMR spectrum of the PVDF-*b*-poly(VAc-*alt*-MAF-TBE) copolymer (Fig. S19) reveals two main signals characteristic of the (i) XA: (-C$\underline{F}_3$ (-71.5 ppm); (ii) VDF[-CH$_2$C$\underline{F}_2$-CH$_2$C$\underline{F}_2$-, normal VDF-VDF dyad addition (-91.5 ppm), (-CH$_2$CF$_2$-CH$_2$CF$_2$-CF$_2$CH$_2$-CH$_2$C$\underline{F}_2$-CH$_2$CF$_2$-, reverse VDF-VDF dyad addition (-95.1 ppm), -CH$_2$C$\underline{F}_2$-CF$_2$CH$_2$-CH$_2$, reverse addition of VDF (−113.9 ppm),[12] -CH$_2$CF$_2$-C$\underline{F}_2$CH$_2$-CH$_2$CH(OAc) (-115.2 ppm, dtt, $^2J_{HF}$ = 55 Hz, $^3J_{HF}$ = 16 Hz and $^4J_{FF}$ = 6 Hz), -CF$_2$-CH$_2$C$\underline{F}_2$-H (-114.3 ppm), chain-end from transfer −CH$_2$CF$_2$−C$\underline{F}_2$CH$_2$−CH$_2$, reverse addition of VDF (-116.2 ppm) and (iii) MAF-TBE (-C$\underline{F}_3$ of MAF-TBE in the copolymer at -67.5 ppm).[16]

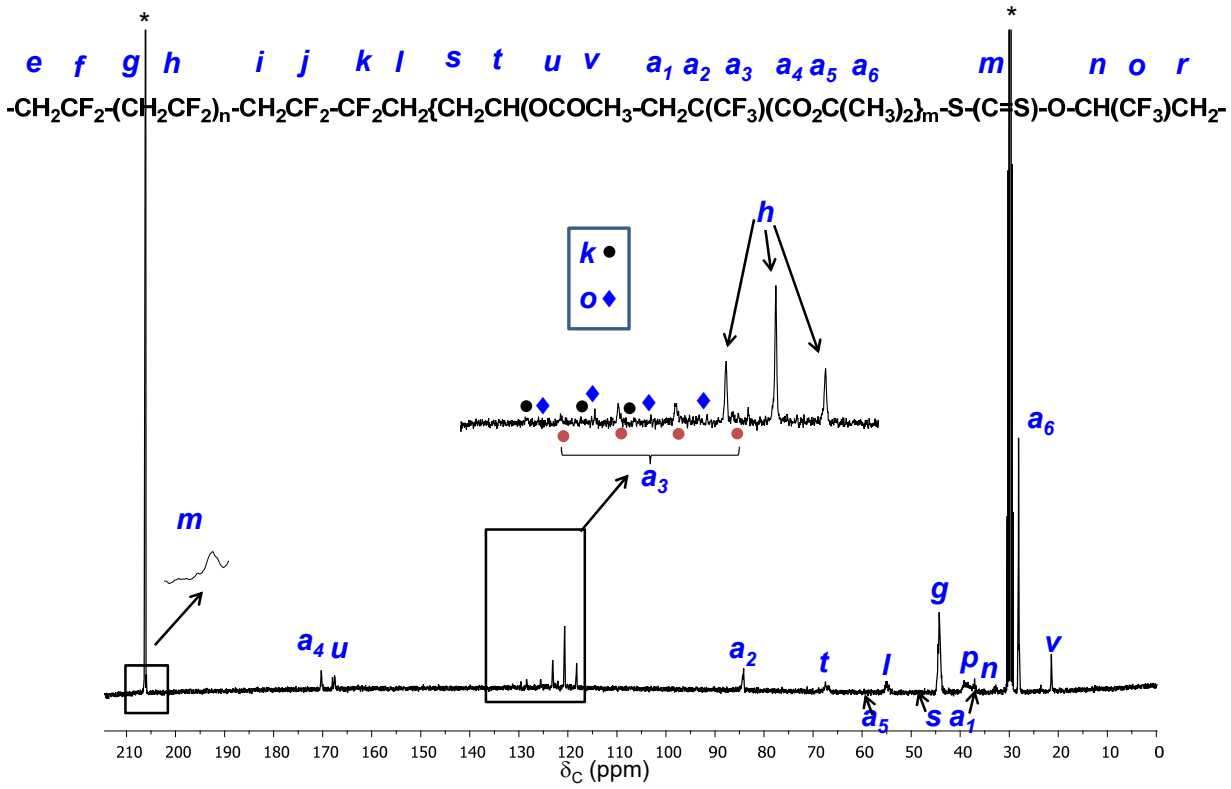

Fig. S20 ^{13}C NMR spectrum of PVDF-*b*-poly(VAc-*alt*-MAF-TBE) (entry P3, Table 1) prepared by RAFT polymerization, recorded in acetone-d_6 at 20 °C. (*) Solvent (acetone) peak.

The ^{13}C NMR spectrum of the PVDF-*b*-poly(VAc-*alt*-MAF-TBE) copolymer (Fig. S20) exhibits the characteristic signal at 21.15 ppm (-OCO<u>C</u>H$_3$ of VAc)[16]; 27.90 ppm {–C(<u>C</u>H$_3$)$_3$ of MAF-TBE}[16]; 32.60 ppm {-O<u>C</u>(CF$_3$)CH$_2$ of XA}; 37.00 ppm {-OCH(CF$_3$)<u>C</u>H$_2$ of XA}; 38.85 ppm (-<u>C</u>H$_2$ of VAc and MAF-TBE); 44.35 ppm (-<u>C</u>H$_2$ of VDF); 54.90 ppm {-<u>C</u>(CH$_3$)$_3$ of MAF-TBE}; 67.15 ppm (-<u>C</u>HOAc of VAc in the VAc-MAF-TBE alternating dyad); 84.10 ppm {-CH$_2$<u>C</u>H(CF$_3$)CO$_2$C(CH$_3$)$_3$ of MAF-TBE}; 118.10 to 123.10 {-OCH(<u>C</u>F$_3$)CH$_2$ of XA, q, $^1J_{CF}$ = 250 Hz}; 119.00 to 129.00 –<u>C</u>F$_3$ of MAF-TBE, t, $^1J_{CF}$ = 252 Hz; 119.80 to 127.00 -<u>C</u>F$_2$ of VDF, t, $^1J_{CF}$ = 252 Hz; 123.50 to 130.00 {-CH$_2$CF$_2$-<u>C</u>F$_2$CH$_2$-CH$_2$CH(-OCO<u>C</u>H$_3$)-, t, $^1J_{CF}$ = 270 Hz }; 167.60 (-O<u>C</u>OCH$_3$ of VAc); 170.20 (-<u>C</u>OOC(CH$_3$)$_3$ of MAF-TBE); 206.80 {-O<u>C</u>=S of XA}.

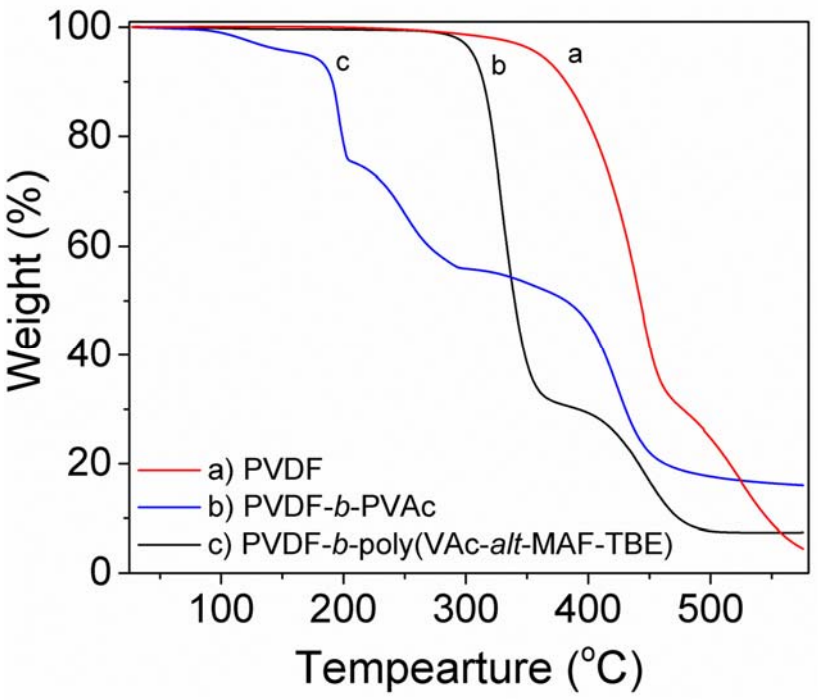

Fig. S21 TGA thermograms of PVDF, PVDF-*b*-PVAc and PVDF-*b*-poly(VAc-*alt*-MAF-TBE) (entries P1-P3, Table S1) multiblock (co)polymers, heated at 10 °C min^{-1} under air.

The thermal properties of the polymers were studied by thermogravimetric analysis (TGA). Expectedly, compared to PVDF, the PVDF-*b*-PVAc block copolymer has lower thermal stability due to the degradation of PVAc.[8] The 25% weight loss of the PVDF-*b*-poly(VAc-*alt*-MAF-TBE) copolymer just above 150 °C (*vs.* no loss for PVDF and PVDF-*b*-PVAc) matches the value calculated for the loss of the carbo-*tert*-butoxy groups in MAF-TBE monomers. It is likely attributed to the *tert*-butyl ester group decomposition into a carboxylic acid group with release of isobutene, followed by a decarboxylation of such a carboxylic acid group.[17] Notably, multiblock PVDF exhibited similar thermal stability (temperature for 10% weight loss, $T_{d,10\%}$ = 390 °C) as the linear PVDF-XA ($T_{d,10\%}$ = 390 °C) prepared by Guerre et al.[8]

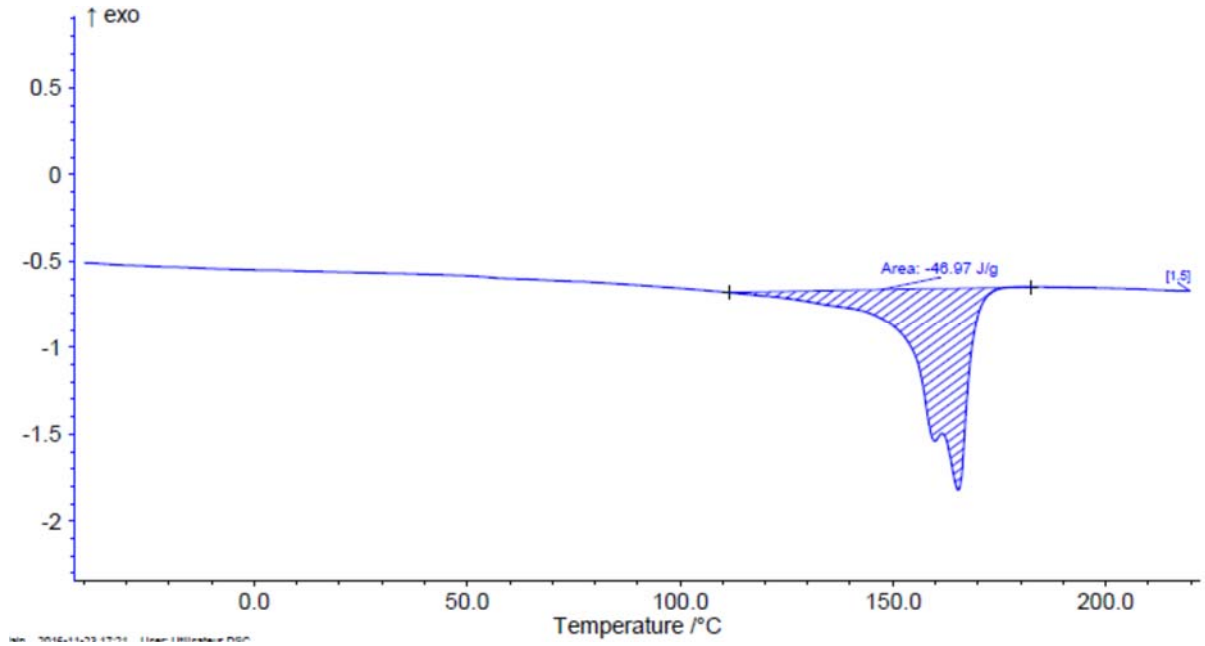

Fig. S22 DSC thermogram of multiblock PVDF (entry P1, Table S1).

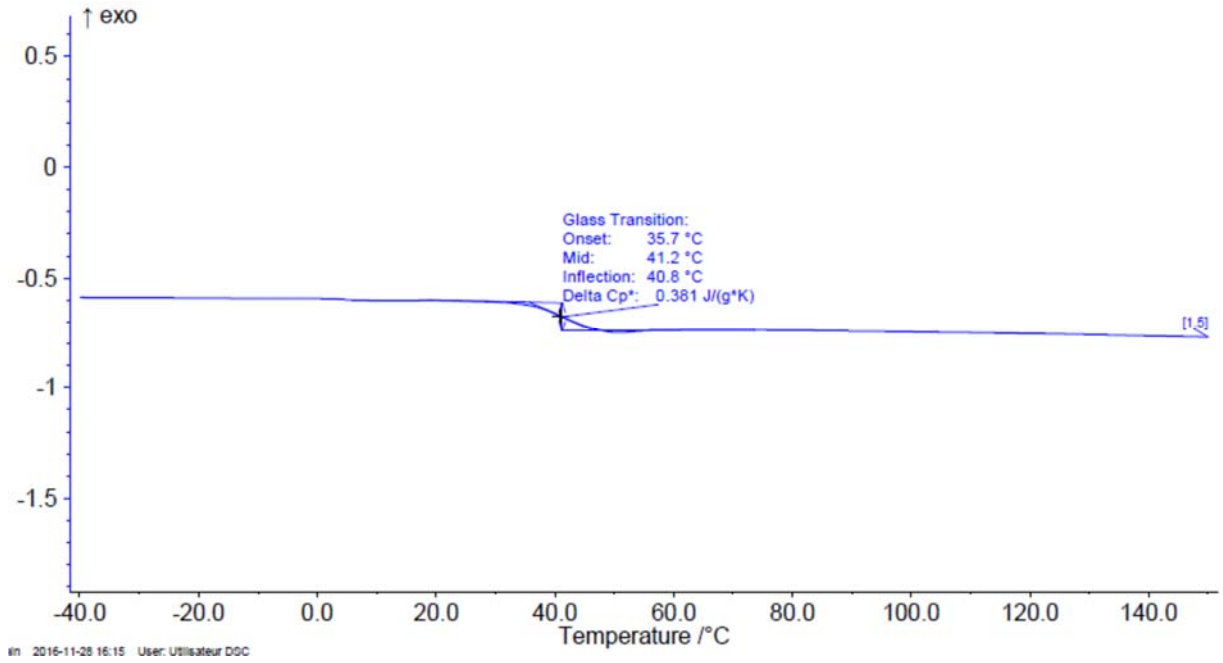

Fig. S23 DSC thermogram of PVDF-*b*-PVAc multiblock copolymer (entry P2, Table S1).

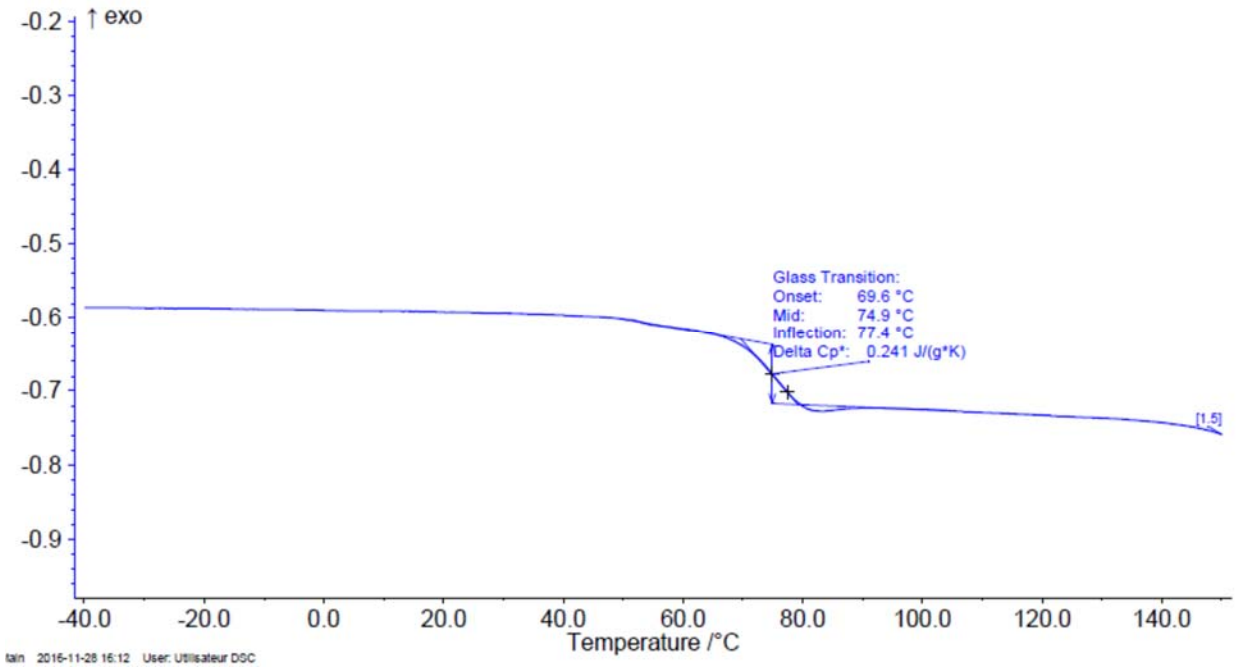

Fig. S24 DSC thermogram of PVDF-*b*-poly(VAc-*alt*-MAF-TBE) multiblock copolymer (entry P3, Table S1).

6- Notes and references

1. V. A. Petrov and W. Marshall, *J. Fluorine Chem.*, 2011, **132**, 41-51.
2. M. Pianca, E. Barchiesi, G. Esposto and S. Radice, *J. Fluorine Chem.*, 1999, **95**, 71-84.
3. Z. Wang, J. He, Y. Tao, L. Yang, H. Jiang and Y. Yang, *Macromolecules*, 2003, **36**, 7446-7452.
4. H. Willcock and R. K. O'Reilly, *Polym. Chem.*, 2010, **1**, 149-157.
5. H. Kise, H. Ogata and M. Nakata, *Angew. Makromolek. Chem.*, 1989, **168**, 205-216.
6. J. Scheirs, *Modern fluoropolymers: High performance polymers for diverse applications*, Wiley, Chichester, 1997.
7. A. Taguet, L. Sauguet, B. Ameduri and B. Boutevin, *J. Fluorine Chem.*, 2007, **128**, 619-630.
8. M. Guerre, S. M. Wahidur Rahaman, B. Ameduri, R. Poli and V. Ladmiral, *Polym. Chem.*, 2016, **7**, 6918-6933.
9. K. Nakagawa and Y. Ishida, *J . Polym. Sci. Part B: Polym. Phys.*, 1973, **11**, 2153-2171.
10. M. Duc, B. Ameduri, B. Boutevin, M. Kharroubi and J.-M. Sage, *Macromol. Rapid Commun.*, 1998, **199**, 1271-1289.
11. M. Guerre, G. Lopez, T. Soulestin, C. Totée, B. Améduri, G. Silly and V. Ladmiral, *Macromol. Chem. Phys.*, **217**, 2016, 2275−2285.
12. M. Guerre, B. Campagne, O. Gimello, K. Parra, B. Ameduri and V. Ladmiral, *Macromolecules*, **48**, 2015, 7810-7822.
13. M. Destarac, W. Bzducha, D. Taton, I. Gauthier-Gillaizeau and S. Z. Zard, *Macromol. Rapid Commun.*, 2002, **23**, 1049-1054.

14. K. Koumura, K. Satoh, M. Kamigaito and Y. Okamoto, *Macromolecules*, 2006, **39**, 4054-4061.

15. A. Debuigne, Y. Champouret, R. Jerome, R. Poli and C. Detrembleur, *Chem. Eur. J.*, 2008, **14**, 4046-4059.

16. S. Banerjee, I. Domenichelli and B. Ameduri, *ACS Macro Lett.*, 2016, **5**, 1232-1236.

17. M. N. Wadekar, Y. R. Patil and B. Ameduri, *Macromolecules*, 2014, **47**, 13-25.